

IMPLICATIONS OF PRECISION ELECTROWEAK DATA

KAORU HAGIWARA

*Theory Group, KEK**Oho, Tsukuba, Ibaraki 305, Japan*

ABSTRACT

There are two aspects to the 1995 summer update of the combined preliminary electroweak data from LEP and SLC. On the one hand, agreement between experiments and the Standard Model (SM) has improved for the line-shape and the asymmetry data. The τ widths and asymmetries are now consistent with $e-\mu-\tau$ universality, and all the asymmetry data including the left-right asymmetry from SLC are consistent with the SM (16%CL). On the other hand, a discrepancy between experiments and SM predictions is sharpened for two observables, R_b and R_c , where R_q is the partial Z boson width ratio Γ_q/Γ_h . R_b is 3% larger (3.7σ) and R_c is 11% smaller (2.5σ) than the SM predictions. When combined, the SM is ruled out at the 99.99%CL for $m_t > 170\text{GeV}$. It is difficult to interpret the $11 \pm 4\%$ deficit of R_c , since if we allow only Γ_b and Γ_c to deviate from the SM then the precisely measured ratio $R_h = \Gamma_h/\Gamma_\ell$ forces the QCD coupling to be $\alpha_s \equiv \alpha_s(m_Z)_{\overline{\text{MS}}} = 0.185 \pm 0.041$, which is uncomfortably large. The data can be consistent with the preferred α_s ($0.10 < \alpha_s < 0.13$) only if the sum $\Gamma_h = \Sigma_q \Gamma_q$ does not deviate significantly from the SM prediction. Possible experimental causes for the under-estimation of R_c are discussed. By assuming the SM value for R_c , the discrepancy in R_b decreases to 2% (3σ). The double tagging technique used for the R_b measurements is critically reviewed. A few theoretical models that can explain large R_b and small α_s ($= 0.104 \pm 0.008$) are discussed. If the QCD coupling α_s is allowed to be fitted by the data, the standard S , T , U analysis for a new physics search in the gauge-boson propagator corrections does not suffer from the R_b and R_c crisis. No signal of new physics is found in the S , T , U analysis once the SM contributions with $m_t \sim 175\text{GeV}$ has been accounted for. The naive QCD-like technicolor model is now ruled out at the 99%CL even for the minimal model with $\text{SU}(2)_{\text{TC}}$. By assuming that no new physics effect is significant in the electroweak observables, we obtain constraints on m_t and m_H as a function of α_s and $\bar{\alpha}(m_Z^2)$, the QED coupling constant at the m_Z scale. A lighter Higgs boson $m_H \lesssim 200\text{GeV}$ is preferred if $m_t < 170\text{GeV}$. The controversy in $\bar{\alpha}(m_Z^2)$ is overcome. However, further improvements in our knowledge of its numerical value is essential in order for the electroweak precision experiments to be sensitive to new physics effects in quantum corrections.

*Talk presented at XVII International Symposium on Lepton and Photon Interactions
at High Energies, 10-15 August 1995, Beijing, China*

IMPLICATIONS OF PRECISION ELECTROWEAK DATA

KAORU HAGIWARA

Theory Group, KEK

Oho, Tsukuba, Ibaraki 305, Japan

ABSTRACT

There are two aspects to the 1995 summer update of the combined preliminary electroweak data from LEP and SLC. On the one hand, agreement between experiments and the Standard Model (SM) has improved for the line-shape and the asymmetry data. The τ widths and asymmetries are now consistent with $e-\mu-\tau$ universality, and all the asymmetry data including the left-right asymmetry from SLC are consistent with the SM (16%CL). On the other hand, a discrepancy between experiments and SM predictions is sharpened for two observables, R_b and R_c , where R_q is the partial Z boson width ratio Γ_q/Γ_h . R_b is 3% larger (3.7σ) and R_c is 11% smaller (2.5σ) than the SM predictions. When combined, the SM is ruled out at the 99.99%CL for $m_t > 170\text{GeV}$. It is difficult to interpret the $11 \pm 4\%$ deficit of R_c , since if we allow only Γ_b and Γ_c to deviate from the SM then the precisely measured ratio $R_h = \Gamma_h/\Gamma_\ell$ forces the QCD coupling to be $\alpha_s \equiv \alpha_s(m_Z)_{\overline{\text{MS}}} = 0.185 \pm 0.041$, which is uncomfortably large. The data can be consistent with the preferred α_s ($0.10 < \alpha_s < 0.13$) only if the sum $\Gamma_h = \Sigma_q \Gamma_q$ does not deviate significantly from the SM prediction. Possible experimental causes for the under-estimation of R_c are discussed. By assuming the SM value for R_c , the discrepancy in R_b decreases to 2% (3σ). The double tagging technique used for the R_b measurements is critically reviewed. A few theoretical models that can explain large R_b and small α_s ($= 0.104 \pm 0.008$) are discussed. If the QCD coupling α_s is allowed to be fitted by the data, the standard S , T , U analysis for a new physics search in the gauge-boson propagator corrections does not suffer from the R_b and R_c crisis. No signal of new physics is found in the S , T , U analysis once the SM contributions with $m_t \sim 175\text{GeV}$ has been accounted for. The naive QCD-like technicolor model is now ruled out at the 99%CL even for the minimal model with $\text{SU}(2)_{\text{TC}}$. By assuming that no new physics effect is significant in the electroweak observables, we obtain constraints on m_t and m_H as a function of α_s and $\bar{\alpha}(m_Z^2)$, the QED coupling constant at the m_Z scale. A lighter Higgs boson $m_H \lesssim 200\text{GeV}$ is preferred if $m_t < 170\text{GeV}$. The controversy in $\bar{\alpha}(m_Z^2)$ is overcome. However, further improvements in our knowledge of its numerical value is essential in order for the electroweak precision experiments to be sensitive to new physics effects in quantum corrections.

1. Introduction

Despite the overwhelming success of the Standard Model (SM) of the electroweak interactions when confronted with experimental observations, there has been a strong and steady belief that the SM is merely an effective low energy description of a more fundamental theory. Moreover, naturalness of the dynamics of the electroweak gauge symmetry breakdown suggests that the energy scale of new physics beyond the SM should lie below or at $\sim 1\text{ TeV}$. This is so whether its last missing ingredient, the Higgs boson, exists or not. It has therefore been hoped that hints of new physics beyond

the SM may be found as quantum effects affecting precision electroweak observables.

In response to such general expectations, the experimental accuracy of the electroweak measurements has steadily been improved in the past several years, reaching the 10^{-5} level for m_Z , a few $\times 10^{-3}$ level for the total and some of the partial Z widths, and 10^{-2} level for the asymmetries at LEP and SLC. Because of partial cancellation in the observable asymmetries at LEP and SLC, their measurements at the 10^{-2} level determine the effective electroweak mixing parameter $\sin^2 \theta_W$ at the 10^{-3} level. Therefore, by choosing the fine structure constant, α , the muon-decay constant G_F , and m_Z as the three inputs whose measurement error is negligibly small, we can test the predictions of the SM at a few $\times 10^{-3}$ level. Accuracy of experiments has now reached the level where new physics contributions to quantum corrections can be probed.

The precision electroweak measurements which were reported as preliminary results for the 1995 Summer Conferences [1,2] are, however, characterized by the following two conflicting aspects.

On the one hand, *all* the observables that were measured at a few $\times 10^{-3}$ level are in perfect agreement with the predictions of the SM. We find no hint of new physics there, and the data are starting to constrain the Higgs boson mass, m_H , in the minimal SM framework provided the top-quark mass, m_t , will be known accurately in the future. The precision of these tests has already reached the level where the present uncertainty of 0.7×10^{-3} [3] in the running QED coupling constant at the m_Z scale, $\bar{\alpha}(m_Z^2)$, is no longer negligible as compared to the other experimental errors which have been attained at LEP and SLC.

On the other hand, significant deviations from the SM predictions are found for the two ratios of the Z partial widths, $R_b = \Gamma(Z \rightarrow 'b\bar{b}')/\Gamma(Z \rightarrow \text{hadrons})$ and $R_c = \Gamma(Z \rightarrow 'c\bar{c}')/\Gamma(Z \rightarrow \text{hadrons})$, which are measured at the 1% and 4% level, respectively. The disagreements are significant, more than $3\text{-}\sigma$ for R_b and more than $2\text{-}\sigma$ for R_c . When combined, the SM can be ruled out at 99.99%CL for $m_t > 170$ GeV [4].

Our task is hence to try to find a consistent picture of electroweak physics that can accommodate simultaneously the above two features of the most recent precision experiments. I would like to report difficulties that I encountered during this course of studies.

The report is organized as follows. In section 2 we summarize the preliminary results [1,2] of the electroweak measurements at LEP and SLC, reported at this Symposium [4]. These data are then compared with the SM predictions [5], and a few remarkable features are pointed out. In section 3 we discuss the nature of the R_b and R_c crisis in detail, and we show that its resolution is intimately related to the possible problem of the magnitude of the strong coupling constant, $\alpha_s \equiv \alpha_s(m_Z)_{\overline{\text{MS}}}$. In particular, it is pointed out that the data on R_c imply too large an α_s in conflict with its recent measurements [6], if the Z partial widths into light quarks (u , d , s) were consistent with the SM predictions. If, on the other hand, we assume the

SM value for R_c , then the data on R_b implies $\alpha_s \sim 0.11$ which is consistent with the estimates from the low-energy experiments. A few theoretical ideas that could explain the R_b data are briefly discussed. In section 4 we perform the comprehensive fit to all the electroweak data by allowing the three parameters [7] S , T , U characterizing possible new physics contributions through the electroweak gauge-boson propagator corrections to vary. Although we assume the SM value for R_c in this analysis, the effects of the new R_b data on this general fit are studied carefully. The simple QCD-like Techni-Color (TC) model is ruled out at the 99%CL even for the minimal model despite the R_b data if we allow α_s to be varied in the fit. The uncertainty in the running QED coupling constant at the m_Z scale, $\bar{\alpha}(m_Z^2)$, is shown as the serious limiting factor for future improvements in the measurement of the S parameter. In section 5 we perform the minimal SM fit to all the electroweak data. Here, despite the R_b and R_c problem, all the electroweak data taken together is consistent with the SM at a few to several %CL for preferred ranges of (m_t, m_H) and α_s . This is a consequence of the excellent agreement between the SM predictions and the rest of the precision data. We show constraints on (m_t, m_H) as functions of α_s and $\bar{\alpha}(m_Z^2)$. Improved numerical precision for the above two coupling constants is essential to improve the constraint on m_H in the minimal SM, and hence to detect new physics effects in quantum corrections. Finally, the quantitative significance of the fermionic and the bosonic radiative corrections is discussed briefly. Section 6 summarizes our findings.

2. Precision Electroweak Data

Table 1 summarizes the results of the LEP Electroweak Working Group [1, 2], which are obtained by combining preliminary electroweak data from LEP, SLC and Tevatron. Correlation matrices among the errors of the line-shape parameters and the heavy-quark parameters are given in Tables 2 and 3, respectively. The errors and their correlations were obtained by combining statistical and systematic errors of individual experiments. All the numerical results presented in this report are obtained by using the data in Tables 1–3, unless otherwise stated.

Also shown in Table 1 are the SM predictions [5] for $m_t = 175$ GeV, $m_H = 100$ GeV, $\alpha_s(m_Z) = 0.12$ and $1/\bar{\alpha}(m_Z^2) = 128.75$. We will discuss implications of the QCD and QED running coupling strengths in sections 3 and 4, respectively. The right-most column gives the difference between the mean of the data and the corresponding SM prediction in units of the experimental error. The data and the SM predictions agree well for most of the observables except for the two ratios R_b and R_c which are, respectively, the partial Z decay widths into $b\bar{b}$ - and $c\bar{c}$ -initiated hadronic states, Γ_b and Γ_c , divided by the Z hadronic decay width Γ_h . R_b is larger than the SM prediction by 3.7- σ , whereas R_c is smaller than the prediction by 2.5- σ . The trends of larger R_b and smaller R_c existed in the combined data for the past few

Table 1. Preliminary electroweak results from LEP, SLC and Tevatron for the 1995 summer conferences [1, 2]. The SM predictions [5] are given for $m_t = 175$ GeV, $m_H = 100$ GeV, $\alpha_s(m_Z) = 0.12$, and [3, 5] $1/\bar{\alpha}(m_Z^2) = 128.75$. See section 4 for the definition of $\bar{\alpha}(m_Z^2)$. Heavy flavor results are obtained by combining data from LEP and SLC [2].

	data	SM	$\frac{\langle \text{data} \rangle - \text{SM}}{(\text{error})}$
LEP			
line shape:			
m_Z (GeV)	91.1884 ± 0.0022	—	—
Γ_Z (GeV)	2.4963 ± 0.0032	2.4985	-0.7
σ_h^0 (nb)	41.488 ± 0.078	41.462	0.3
$R_\ell \equiv \Gamma_h / \Gamma_\ell$	20.788 ± 0.032	20.760	0.9
$A_{\text{FB}}^{0,\ell}$	0.0172 ± 0.0012	0.0168	0.4
τ polarization:			
A_τ	0.1418 ± 0.0075	0.1486	-0.9
A_e	0.1390 ± 0.0089	0.1486	-1.1
heavy flavor results:			
$R_b \equiv \Gamma_b / \Gamma_h$	0.2219 ± 0.0017	0.2157	3.7
$R_c \equiv \Gamma_c / \Gamma_h$	0.1540 ± 0.0074	0.1722	-2.5
$A_{\text{FB}}^{0,b}$	0.0997 ± 0.0031	0.1041	-1.4
$A_{\text{FB}}^{0,c}$	0.0729 ± 0.0058	0.0746	-0.3
$q\bar{q}$ charge asymmetry:			
$\sin^2 \theta_{\text{eff}}^{\text{lept}} (\langle Q_{FB} \rangle)$	0.2325 ± 0.0013	0.2313	0.9
SLC			
A_{LR}^0	0.1551 ± 0.0040	0.1486	1.6
A_b	0.841 ± 0.053	0.935	-1.8
A_c	0.606 ± 0.090	0.669	-0.7
$p\bar{p}$			
m_W	80.26 ± 0.16	80.40	0.9

years, but their significance grew considerably in the updated data.

Before starting discussions on the implications of the new R_b and R_c data in section 3, I would like you to keep in mind the following three observations:

- The three line-shape parameters, Γ_Z , σ_h^0 and R_ℓ , are now measured with accu-

Table 2. The error correlation matrix for the Z line-shape parameters [1].

	m_Z	Γ_Z	σ_h^0	R_ℓ	$A_{\text{FB}}^{0,\ell}$
m_Z	1.00	-0.08	0.02	0.00	0.08
Γ_Z	-0.08	1.00	-0.12	-0.01	0.00
σ_h^0	0.02	-0.12	1.00	0.15	0.01
R_ℓ	0.00	-0.01	0.15	1.00	0.00
$A_{\text{FB}}^{0,\ell}$	0.08	0.00	0.01	0.00	1.00

Table 3. The error correlation matrix for the b and c quark results [2].

	R_b	R_c	$A_{\text{FB}}^{0,b}$	$A_{\text{FB}}^{0,c}$	A_b	A_c
R_b	1.000	-0.345	0.005	0.055	-0.068	0.046
R_c	-0.345	1.000	0.084	-0.063	0.074	-0.061
$A_{\text{FB}}^{0,b}$	0.005	0.084	1.000	0.109	0.062	-0.025
$A_{\text{FB}}^{0,c}$	0.055	-0.063	0.109	1.000	-0.018	0.073
A_b	-0.068	0.074	0.062	-0.018	1.000	0.074
A_c	0.046	-0.061	-0.025	0.073	0.074	1.000

racy better than 0.2%.

$$\frac{\Delta\Gamma_Z}{\Gamma_Z} = -0.0010 \pm 0.0013, \quad (1a)$$

$$\frac{\Delta\sigma_h^0}{\sigma_h^0} = 0.0006 \pm 0.0019, \quad (1b)$$

$$\frac{\Delta R_l}{R_l} = 0.0015 \pm 0.0015 \quad (1c)$$

where Δ gives the difference between the data and the SM predictions of Table 1. It is important to note that these high accuracy data are sensitive to quantum effects and that any attempted modification of the SM should pass these tests.

- I show in the Tables only the results obtained by assuming the e - μ - τ universality, because detailed tests [1, 4] show that a hint of universality violation in the τ -data is disappearing.

$$\frac{\Delta\Gamma_\tau}{\Gamma_\tau} = 0.000 \pm 0.0035, \quad (2a)$$

$$\frac{\Delta A_\tau}{A_\tau} = -0.04 \pm 0.05, \quad (2b)$$

$$\frac{\Delta A_{\text{FB}}^\tau}{A_{\text{FB}}^\tau} = 0.23 \pm 0.14. \quad (2c)$$

Although the τ Forward-Backward asymmetry is still 1.7σ away from the SM prediction the accuracy of the measurement is still poor and its significance is overshadowed by excellent agreements in the partial width Γ_τ and the τ polarization asymmetry which are measured at the 0.35% and 5% level, respectively.

- All the asymmetry data, including the left-right beam-polarization asymmetry, A_{LR} , from SLC, are now consistent with each other. I show in Fig. 1 the result of the one-parameter fit to all the asymmetry data in terms of the effective electroweak mixing angle, $\bar{s}^2(m_Z^2)$ [5], which is numerically related to the effective parameter $\sin^2\theta_{\text{eff}}^{\text{lept}}$ adopted by the LEP group [1] as $\bar{s}^2(m_Z^2) = \sin^2\theta_{\text{eff}}^{\text{lept}} - 0.0010$ [5], within the SM. The fit gives

$$\bar{s}^2(m_Z^2) = 0.23039 \pm 0.00029 \quad (3)$$

with $\chi_{\text{min}}^2/(\text{d.o.f.}) = 13.0/(9)$. The updated measurements of the asymmetries agree well (16%CL) with the ansatz that the asymmetries are determined by the universal electroweak mixing parameter.

In concluding the section, I would like to point out that the electroweak data of Tables 1–3 all together are still consistent with the reference predictions of the SM

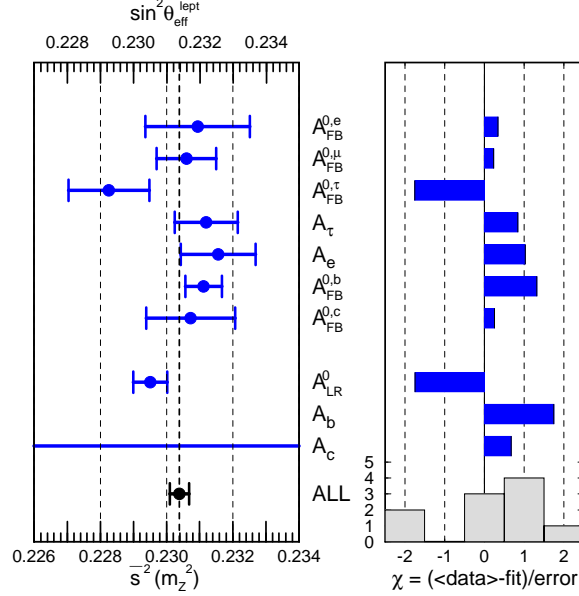


Fig. 1. The effective electroweak mixing parameter $\bar{s}^2(m_Z^2)$ is determined from all the asymmetry data from LEP and SLC. The effective parameter $\sin^2 \theta_{\text{eff}}^{\text{lept}}$ of the LEP Electroweak Working Group [1] is related to $\bar{s}^2(m_Z^2)$ as [5] $\sin^2 \theta_{\text{eff}}^{\text{lept}} = \bar{s}^2(m_Z^2) + 0.0010$. The data on A_b is off the scale.

shown in Table 1 at the 3%CL. The low confidence level can be traced back to the poor agreement of the measured and predicted values for R_b and R_c . It does not improve significantly by varying the SM parameters if we respect the m_t bounds from the Tevatron experiments [8, 9] which typically give $160 \text{ GeV} \lesssim m_t \lesssim 200 \text{ GeV}$.

3. The R_b and R_c Crisis and α_s

The most striking results of the updated electroweak data are those of R_b and R_c , which are shown in Fig. 2. The SM predictions to these ratios are shown by the thick solid line, where the top-quark mass in the $Zb_L b_L$ vertex correction is indicated by solid blobs. When combined the R_b and R_c data alone reject the SM at the 99.99%CL. The thin solid line represents the prediction of the extended SM where in the $Zb_L b_L$ vertex function [5],

$$\Gamma_L^{Zbb}(q^2) = -\hat{g}_Z \left\{ -\frac{1}{2} [1 + \bar{\delta}_b(q^2)] + \frac{1}{3} \hat{s}^2 [1 + \Gamma_1^{b_L}(q^2)] \right\}, \quad (4)$$

the function $\bar{\delta}_b(m_Z^2)$ is allowed to take an arbitrary value. Here $\hat{g}_Z \equiv \hat{g}/\hat{c} \equiv \hat{e}/\hat{s}\hat{c}$ are properly renormalized $\overline{\text{MS}}$ couplings [5]. In the SM, the function $\bar{\delta}_b(m_Z^2)$ always takes a negative value ($\bar{\delta}_b(m_Z^2) \lesssim -0.03$) and its magnitude grows quadratically with m_t . It can be parametrized accurately in the region $100 < m_t (\text{GeV}) < 200$ as [5]

$$\bar{\delta}_b(m_Z^2)_{\text{SM}} \approx -0.00099 - 0.00211 \left(\frac{m_t + 31}{100} \right)^2. \quad (5)$$

The data are not only inconsistent with the SM but also inconsistent at more than the 2- σ level with its extension where only the Zb_Lb_L vertex function is modified.

The correlation between the two observables, R_b and R_c , can be understood as follows [2, 4]: To a good approximation, the measurement of R_c does not depend on the assumed value of R_b , because it is measured by detecting leading charmed-hadrons in a leading-jet for which a b-quark jet rarely contributes. On the other hand, the measurement of R_b is affected by the assumed value of R_c , since it typically makes use of its decay-in-flight vertex signal for which charmed particles can also contribute. We find that the following parametrization,

$$R_b = 0.2205 - 0.0136 \frac{R_c - 0.172}{0.172} \pm 0.0016, \quad (6a)$$

$$R_c = 0.1540 \pm 0.0074, \quad (6b)$$

reproduces the correlation obtained by the data of Tables 1 and 3 excellently, as indicated by the shaded regions in Fig. 2. Note that we give a 39%CL contour in all of the two-parameter fits so that the projected 1- σ errors can easily be read off.

Before discussing the implications of this striking result, we should remind the fact that the three most accurately measured line-shape parameters in Eq.(1) determine the Z partial widths Γ_l , Γ_h and Γ_{inv} accurately,

$$\Delta\Gamma_h/\Gamma_h = 0.0001 \pm 0.0017, \quad (7a)$$

$$\Delta\Gamma_l/\Gamma_l = -0.0013 \pm 0.0016, \quad (7b)$$

$$\Delta\Gamma_{\text{inv}}/\Gamma_{\text{inv}} = -0.004 \pm 0.005, \quad (7c)$$

because they are three independent combinations of the above three widths, $\Gamma_Z = \Gamma_h + 3\Gamma_l + \Gamma_{\text{inv}}$, $R_l = \Gamma_h/\Gamma_l$, and $\sigma_h^0 = (12\pi/m_Z^2)\Gamma_h\Gamma_l/\Gamma_Z^2$. That the hadronic Z

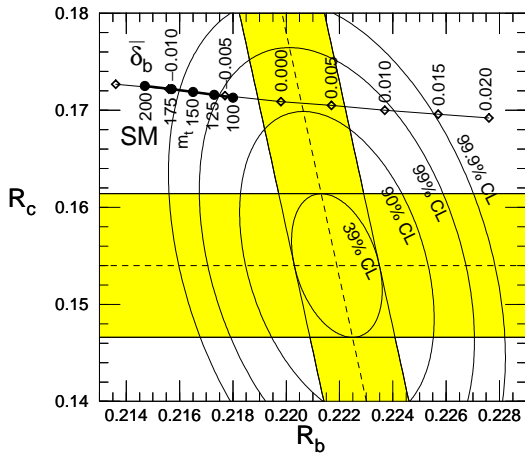


Fig. 2. R_b and R_c data [2] and the SM predictions [5].

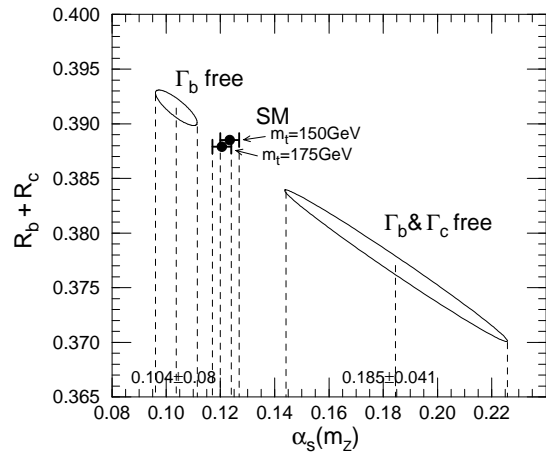


Fig. 3. $R_b + R_c$ vs α_s .

partial width, Γ_h , is measured with 0.17% accuracy strongly constrains our attempt to modify theoretical predictions for the ratios R_b and R_c . This is because Γ_h can be approximately expressed as

$$\begin{aligned}\Gamma_h &= \Gamma_u + \Gamma_d + \Gamma_s + \Gamma_c + \Gamma_b + \Gamma_{\text{others}} \\ &\sim \{\Gamma_u^0 + \Gamma_d^0 + \Gamma_s^0 + \Gamma_c^0 + \Gamma_b^0\} \times [1 + \frac{\alpha_s}{\pi} + \mathcal{O}(\frac{\alpha_s}{\pi})^2],\end{aligned}\quad (8)$$

where Γ_q^0 's are the partial widths in the absence of the final state QCD corrections. Hence, to a good approximation, the ratios R_q can be expressed as ratios of Γ_q^0 and their sum. A decrease in R_b and an increase in R_c should then imply a decrease and an increase of Γ_b^0 and Γ_c^0 , respectively, from their SM predicted values. In order to satisfy the experimental constraint on Γ_h one should hence adjust the α_s value in Eq.(8).

The consequence of this constraint is clearly shown in Fig. 3 where, once we allow *both* Γ_b^0 and Γ_c^0 to be freely fitted by the data, the above Γ_h constraint forces α_s to be unacceptably large. On the other hand, if we allow only Γ_b^0 to vary by assuming the SM value of Γ_c^0 (the straight line of the extended SM in Fig. 2), then the Γ_h constraint gives a slightly small value of α_s , which is compatible [5, 10] with some of the low-energy measurements [11, 12] and lattice QCD estimates [13, 14]. Although the SM does not reproduce the R_b and R_c data it gives a moderate α_s value consistent with the estimates based on the e^+e^- jet-shape measurements [6, 15] and the hadronic τ -decay rate [6]. Although the τ -decay measurement has the smallest experimental and perturbative-QCD error it may still suffer from non-perturbative corrections [16], and a larger theoretical uncertainty may be assigned [17]: see Fig. 4.

In fact we do not yet have a definite clue where in the region $0.105 < \alpha_s(m_Z) < 0.125$ the true QCD coupling constant lies. $\alpha_s \sim 0.12$ is favored from the electroweak data, if we believe in the SM predictions for R_b and R_c despite the strong experimental signals. On the other hand $\alpha_s \sim 0.11$ is favored if we believe in the SM predictions for Γ_c^0 while allowing new physics to modify Γ_b^0 . These two solutions both lead to an acceptable α_s value at present. However, once we allow new physics in both Γ_b^0 and Γ_c^0 and let them be fitted by the data, then an unacceptably large α_s follows.

In fact, if we stick to the very conservative bounds $0.105 < \alpha_s(m_Z) < 0.125$, we cannot explain the discrepancies in both R_b and R_c by allowing new physics only in Γ_b^0 and Γ_c^0 . The only sensible solution, then, may be to allow a new physics contribution to all Γ_q^0 such that their sum stays roughly at the SM value, e.g. by making all the down-type-quark widths larger than their SM values by 3% and the up-type-quark widths to be smaller by 6%. Such a model would explain both R_b and R_c , and give a reasonable α_s . It is not easy to find a working model, however, which does not jeopardize all the excellent successes of the SM in the quark and lepton asymmetries, the leptonic widths, m_W , and in the low-energy neutral-current data.

Because the R_c measurement depends strongly on the charm-quark detection efficiency, which has uncertainties in charmed-quark fragmentation function into

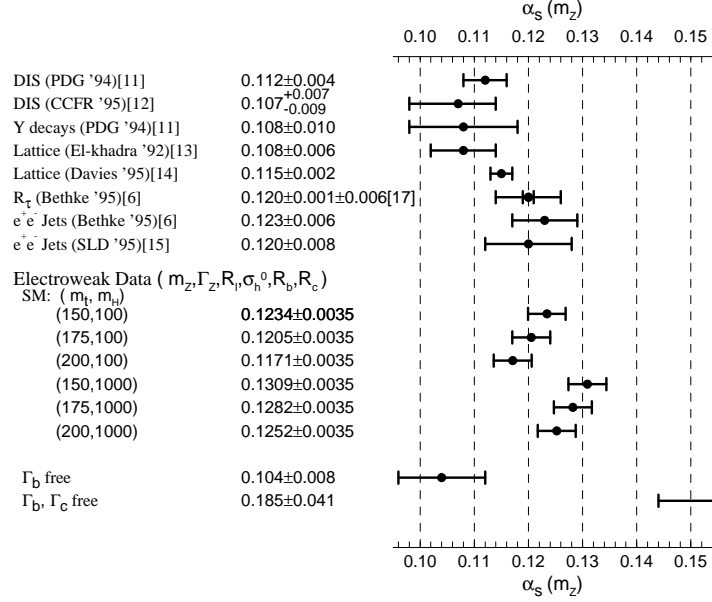


Fig. 4. Compilation of α_s values as measured by various experiments and by Lattice QCD calculations.

charmed hadrons and in charmed-hadron decay branching fractions, it is still possible that unexpected errors are hiding. As an extreme example, if as much as 10% of the charmed-quark final states were unaccounted for, then *both* the 10% deficit in R_c at LEP *and* the 10% too few charmed hadron multiplicity in B-meson decays [18, 19] can be solved.

If we assume that R_c actually has the SM value $R_c \sim 0.172$ and temporarily set aside its experimental constraint, then the correlation as depicted by Eq.(6a) tells that the measured $R_b = 0.2205 \pm 0.0016$ is about 2% larger than the SM prediction, $R_b \sim 0.216$ for $m_t \sim 175$ GeV. The discrepancy is still significant at the 3- σ level.

I examined the possibility that an experimental problem that could result in an underestimation of R_c can lead to an overestimation of R_b . This does not seem to be the case, since R_b is measured mainly by using a different technique, the double-tagging method [4], where the b -quark tagging efficiency is determined experimentally rather than by estimating it from the b -quark fragmentation model and the b -flavored hadron decay rates. Schematically the single and double b -tag event rate in hadronic two-jet events are expressed as

$$\frac{N_T}{2N_h} = \epsilon_b r_b R_b + \epsilon_c r_c R_c + \text{others}, \quad (9a)$$

$$\frac{N_{TT}}{N_h} = C \{ \epsilon_b^2 r_b R_b + \epsilon_c^2 r_c R_c + \text{others} \}, \quad (9b)$$

where ϵ_q denotes the efficiency of tagging a q -jet, r_q is the rate of two-jet-like events ($T > 0.8$) in the $q\bar{q}$ initiated events, and deviation of C from unity measures possible

correlation effects between two jets. By choosing the tagging condition such that $\epsilon_b \gg \epsilon_c$, one can self-consistently determine both ϵ_b and R_b :

$$R_b = \frac{C}{r_b} \frac{[\frac{N_T}{2N_h} - \epsilon_c \frac{r_c}{r_b} R_c - \dots]^2}{[\frac{N_{TT}}{N_h} - \epsilon_c^2 \frac{r_c}{r_b} R_c - \dots]}. \quad (10)$$

In the limit of uncorrelated two-jet events only $C = 1$ and $r_b = 1$, and in the limit of a negligible contribution from non- b events, the ratio R_b is determined from the ratio of the square of the single-tag event rate and the double-tag event rate. Only for the corrections to this limit are the QCD motivated hadron-jet Monte Carlo programs used. A compilation of very careful tests of these correction terms are found in the LEP/SLC Heavy Flavor Group report [2]. We should still examine if our present understanding of generating hadronic final states from quark-gluon states allows us to constrain the coefficients C and r_b at much less than a % level and the miss-tagging efficiency $\epsilon_c \sim 0.01$ at 10% level. For instance, the combination of an overestimation of C by 0.5% with an underestimation of r_b by 0.5% and ϵ_c by 10%, can result in an overestimate of R_b by 2%. Serious theoretical studies of the uncertainty in the present hadron-jet generation program are needed, because in my opinion, these programs have never been tested at the accuracy level that was achieved by these excellent experiments at LEP.

There have been many attempts to explain the discrepancy in R_b by invoking new physics beyond the SM. Most notably, in the minimal supersymmetric (SUSY) SM [20, 21, 22, 23, 24, 25, 26, 27, 28, 29, 30, 31, 32, 33], an additional loop of a light \tilde{t}_R and a light higgsino-like chargino, or that with an additional Higgs pseudoscalar when $\tan \beta \gg 1$, can compensate the large negative top quark contribution of the SM in the $Zb_L b_L$ vertex function. Such a solution typically leads to the prediction that the masses of the lighter \tilde{t} and chargino, or the pseudoscalar should be smaller than m_Z . In the former scenario the top quark should have significant exotic decays into \tilde{t}_R and a neutral Higgsino, and in the latter scenario another exotic decay $t \rightarrow b + H^+$ may occur [27, 30, 31, 32, 33]. In both SUSY scenarios, we should expect to find new particles at Tevatron, LEP2 or even at LEP1.5.

In an alternative scenario of the electroweak symmetry breaking, the Techni-Color (TC) model, the heavy top quark mass implies strong interactions among top-quarks and techniquarks. Such interactions, typically called the extended technicolor (ETC) interactions, can affect the $Zb_L b_L$ vertex. However, the side-ways ETC bosons that connect the top-quark and techniquark leads to a contribution with an opposite sign [34, 35]. The diagonal ETC bosons contribute [36] with the correct sign [37], and their consequences have been studied [38, 39]. The diagonal ETC bosons that explain the R_b data are, however, found [40] to give an unacceptably large contribution to the T parameter [7].

As an alternative to the standard ETC model where the ETC gauge group commutes with the SM gauge group, models with non-commuting ETC gauge group have

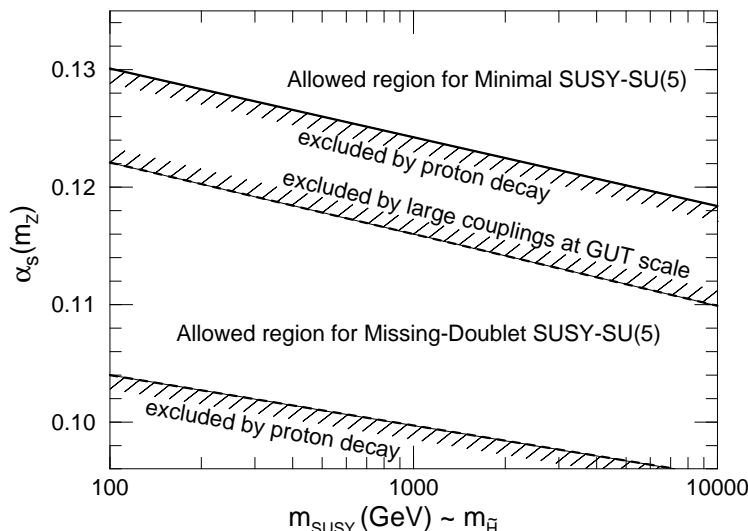


Fig. 5. Constraints on $\alpha_s(m_Z)_{\overline{\text{MS}}}$ as functions of the SUSY threshold scale m_{SUSY} in the minimal SUSY-SU(5) model [44] and in the model with the missing-doublet mechanism [45].

been proposed [41] which have rich phenomenological consequences. It is also noted that an existence of the new heavy gauge boson X that couples only to the third-generation quarks and leptons has been proposed [42], which can affect both the $Zb\bar{b}$ and $Z\tau\tau$ vertices through mixing with the SM Z .

So far, the above models affect mainly the $Zb_L b_L$ coupling, which dominates the $Zb_R b_R$ coupling in the SM. A possible anomaly in the b -jet asymmetry parameter, A_b , observed at SLC with its polarized beam, see Table 1 and Fig. 1, may suggest a new physics contribution in the $Zb_R b_R$ vertex [43]. It is worth watching improved A_b measurements at SLC in the future.

Finally, I would like to note that the small α_s value which is obtained by allowing a new physics contribution to explain the R_b anomaly tends to destroy the SUSY-SU(5) unification of the three gauge couplings in the minimal model [44]. This problem is, however, highly dependent on details of the particle mass spectrum at the GUT scale. In fact in the missing doublet SUSY-SU(5) model [45] which naturally explains the doublet-triplet splitting, smaller α_s is preferred due to its peculiar GUT particle spectrum [46, 47, 48, 49]. I show in Fig. 5 the update [50] for the allowed regions of $\alpha_s(m_Z)$ in the two SUSY-SU(5) models as functions of the heavy Higgsino mass, where the standard supergravity model assumptions are made for the SUSY particle masses at the electroweak scale.

4. Global Fit to All Electroweak Data with S , T , U

In this section we present the results of the global fit to all the electroweak data in which we allow new physics contribution to the S , T , U parameters [7] of the electroweak gauge-boson-propagator corrections as well as to the $Zb_L b_L$ vertex form

factor, $\bar{\delta}_b(m_Z^2)$, but otherwise we assume the SM contribution to dominate the corrections. We take the strengths of the QCD and QED couplings at the m_Z scale, $\alpha_s(m_Z)$ and $\bar{\alpha}(m_Z^2)$, as external parameters of the fits, so that implications of their precise measurements on electroweak physics are manifestly shown.

4.1. Brief Review of Electroweak Radiative Corrections in $SU(2)_L \times U(1)_Y$ Models

The propagator corrections in the general $SU(2)_L \times U(1)_Y$ models can conveniently be expressed in terms of the following four effective charge form-factors [5]:

$$\begin{array}{c} \text{Diagram: } \gamma \text{ line with a loop} \\ \sim \bar{\alpha}(q^2) = \hat{e}^2 \left[1 - \text{Re} \overline{\Pi}_{T,\gamma}^{\gamma\gamma}(q^2) \right], \end{array} \quad (11a)$$

$$\begin{array}{c} \text{Diagram: } \gamma \text{ line with a } Z \text{ loop} \\ \sim \bar{s}^2(q^2) = \hat{s}^2 \left[1 + \hat{s} \hat{c} \text{Re} \overline{\Pi}_{T,\gamma}^{\gamma Z}(q^2) \right] \end{array} \quad (11b)$$

$$\begin{array}{c} \text{Diagram: } Z \text{ line with a } Z \text{ loop} \\ \sim \bar{g}_Z^2(q^2) = \hat{g}_Z^2 \left[1 - \text{Re} \overline{\Pi}_{T,Z}^{ZZ}(q^2) \right], \end{array} \quad (11c)$$

$$\begin{array}{c} \text{Diagram: } W \text{ line with a } W \text{ loop} \\ \sim \bar{g}_W^2(q^2) = \hat{g}^2 \left[1 - \text{Re} \overline{\Pi}_{T,W}^{WW}(q^2) \right], \end{array} \quad (11d)$$

where $\overline{\Pi}_{T,V}^{AB}(q^2) \equiv [\overline{\Pi}_T^{AB}(q^2) - \overline{\Pi}_T^{AB}(m_V^2)]/(q^2 - m_V^2)$ are the propagator correction factors that appear in the S -matrix elements after the mass renormalization is performed, and $\hat{e} \equiv \hat{g} \hat{s} \equiv \hat{g}_Z \hat{s} \hat{c}$ are the $\overline{\text{MS}}$ couplings. The ‘overlines’ denote the inclusion of the pinch terms [51, 53], which make these effective charges useful [53, 5, 54] even at very high energies ($|q^2| \gg m_Z^2$). The amplitudes are then expressed in terms of these charge form-factors plus appropriate vertex and box corrections. Hence the charge form-factors can be directly extracted from the experimental data by assuming SM dominance to the vertex and box corrections, and the extracted values can be compared with various theoretical predictions.

We can define [5] the S , T , and U variables of Ref. [7] in terms these effective charges,

$$\frac{\bar{s}^2(m_Z^2) \bar{c}^2(m_Z^2)}{\bar{\alpha}(m_Z^2)} - \frac{4\pi}{\bar{g}_Z^2(0)} \equiv \frac{S}{4}, \quad (12a)$$

$$\frac{\bar{s}^2(m_Z^2)}{\bar{\alpha}(m_Z^2)} - \frac{4\pi}{\bar{g}_W^2(0)} \equiv \frac{S+U}{4}, \quad (12b)$$

$$1 - \frac{\bar{g}_W^2(0)}{m_Z^2} \frac{m_Z^2}{\bar{g}_Z^2(0)} \equiv \alpha T, \quad (12c)$$

where it is made clear that these variables measure deviations from the naive universality of the electroweak gauge boson couplings. They receive contributions from both the SM radiative effects as well as new physics contributions. The original S , T ,

U variables [7] are obtained [5] approximately by subtracting the SM contributions (at $m_H = 1000$ GeV).

For a given electroweak model we can calculate the S , T , U parameters (T is a free parameter in models without the custodial SU(2) symmetry), and the charge form-factors are then fixed by the following identities [5]:

$$\frac{1}{\bar{g}_Z^2(0)} = \frac{1 + \bar{\delta}_G - \alpha T}{4\sqrt{2}G_F m_Z^2}, \quad (13a)$$

$$\bar{s}^2(m_Z^2) = \frac{1}{2} - \sqrt{\frac{1}{4} - \bar{\alpha}^2(m_Z^2) \left(\frac{4\pi}{\bar{g}_Z^2(0)} + \frac{S}{4} \right)}, \quad (13b)$$

$$\frac{4\pi}{\bar{g}_W^2(0)} = \frac{\bar{s}^2(m_Z^2)}{\bar{\alpha}^2(m_Z^2)} - \frac{1}{4}(S + U). \quad (13c)$$

Here $\bar{\delta}_G$ is the vertex and box correction to the muon lifetime [55] after subtraction of the pinch term [5]:

$$G_F = \frac{\bar{g}_W^2(0) + \hat{g}^2 \bar{\delta}_G}{4\sqrt{2}m_W^2}. \quad (14)$$

In the SM, $\bar{\delta}_G = 0.0055$ [5].

It is clear from the above identities that once we know T and $\bar{\delta}_G$ in a given model we can predict $\bar{g}_Z^2(0)$, and then by knowing S and $\bar{\alpha}(m_Z^2)$ we can calculate $\bar{s}^2(m_Z^2)$, and finally by knowing U we can calculate $\bar{g}_W^2(0)$. Since $\bar{\alpha}(0) = \alpha$ is known precisely, all four charge form factors are fixed at one q^2 point. The q^2 -dependence of the form factors should also be calculated in a given model, but it is less dependent on physics at very high energies [5]. In the following analysis we assume that the SM contribution governs the running of the charge form-factors between $q^2 = 0$ and $q^2 = m_Z^2$. We can now predict all the neutral-current amplitudes in terms of S and T , and an additional knowledge of U gives the W mass via Eq.(14).

We should note here that our prediction for the effective mixing parameter $\bar{s}^2(m_Z^2)$ is not only sensitive to the S and T parameters but also on the precise value of $\bar{\alpha}(m_Z^2)$. This is the reason why our predictions for the asymmetries measured at LEP/SLC and, consequently, the experimental constraint on S extracted from the asymmetry data are dependent on $\bar{\alpha}(m_Z^2)$. In order to parametrize the uncertainty in our evaluation of $\bar{\alpha}(m_Z^2)$, the parameter δ_α is introduced in Ref. [5] as follows: $1/\bar{\alpha}(m_Z^2) \equiv 4\pi/\bar{e}(m_Z^2) = 128.72 + \delta_\alpha$. We show in Table 4 the results of the four recent updates [56, 57, 3, 58] on the hadronic contribution to the running of the effective QED coupling. Three definitions of the running QED coupling are compared. I remark that our simple formulae (11) and (12) are valid only if one includes all the fermionic and bosonic contributions to the propagator corrections.

A more extensive list of the estimates are shown in Fig. 6. The analysis of Ref. [5] was based on the estimate [62], $\delta_\alpha = 0.00 \pm 0.10$. Nevzorov *et al.* [63] made use of

Table 4. The running QED coupling at the m_Z scale in the three schemes. $1/\alpha(m_Z^2)_{\text{l.f.}}$ contains only the light fermion contributions to the running of the QED coupling constant between $q^2 = 0$ and $q^2 = m_Z^2$. $1/\alpha(m_Z^2)_{\text{f}}$ contains all fermion contributions including the top-quark. $m_t = 175$ GeV and $\alpha_s(m_Z) = 0.12$ in the perturbative two-loop correction [59] are assumed. $1/\bar{\alpha}(m_Z^2)$ contains also the W -boson-loop contribution [5] including the pinch term [51, 52].

	$1/\alpha(m_Z^2)_{\text{l.f.}}$	$1/\alpha(m_Z^2)_{\text{f}}$	$1/\bar{\alpha}(m_Z^2)$	δ_α
Martin-Zeppenfeld '94 [56]	128.98 ± 0.06	128.99 ± 0.06	128.84 ± 0.06	0.12 ± 0.06
Swartz '95 [57]	128.96 ± 0.06	128.97 ± 0.06	128.82 ± 0.06	0.10 ± 0.06
Eidelman-Jegerlehner '95 [3]	128.89 ± 0.09	128.90 ± 0.09	128.75 ± 0.09	0.03 ± 0.09
Burkhardt-Pietrzyk '95 [58]	128.89 ± 0.10	128.90 ± 0.10	128.76 ± 0.10	0.04 ± 0.10

perturbative QCD down to $\sqrt{s} \sim 1$ GeV, while the estimates by Geshkenbein and Morgunov [64, 65] are based on a theoretical model of resonance production. Martin and Zeppenfeld [56] also relied on the perturbative QCD, but they restrict its use to constraining only the overall normalization of the data at $\sqrt{s} > 3$ GeV. Their estimate agrees well with the revised evaluation by Swartz [57] who used only experimental data. Finally two of the most recent values [3, 58] agree perfectly. There is no real discrepancy among the four recent estimates in Table 4, where small differences are attributed to the use of perturbative QCD for constraining the magnitude of medium energy data [56] or to a slightly different set of input data [57]. For more detailed discussions I refer the readers to an excellent review by Takeuchi [66]. In the following analysis we take the estimate of Ref. [3] ($\delta_\alpha = 0.03 \pm 0.09$) as the standard, and show sensitivity of our results on $\delta_\alpha - 0.03$.

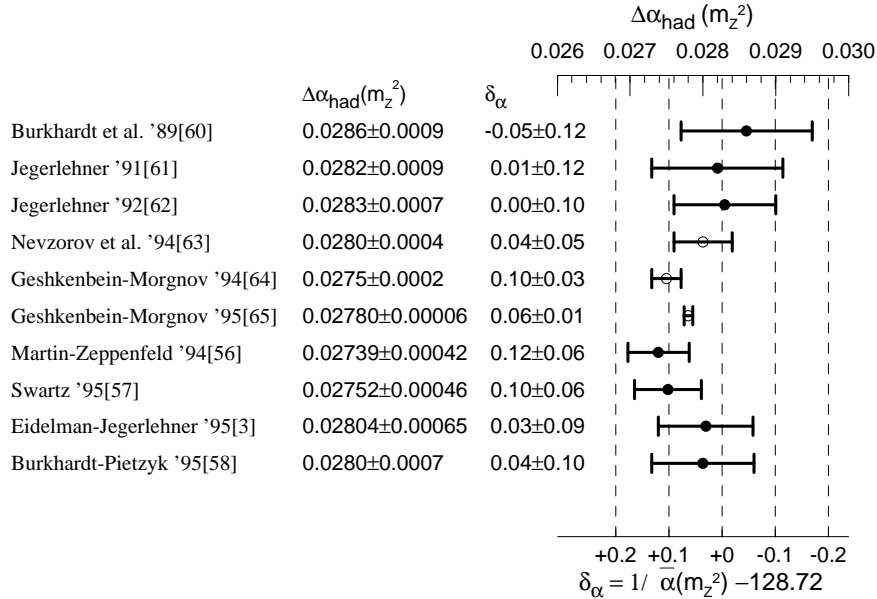


Fig. 6. Various estimates of $\Delta\alpha_{\text{had}}(m_Z^2)$ and the resulting $\bar{\alpha}(m_Z^2)$ in the minimal SM. The parameter δ_α [5] is defined as $\delta_\alpha \equiv 1/\bar{\alpha}(m_Z^2) - 128.72$.

Once we know $\bar{\alpha}(m_Z^2)$ the charge form-factors in Eq.(13) can be calculated from S , T , U . The following approximate formulae [5] are useful:

$$\bar{g}_Z^2(0) \approx 0.5456 + 0.0040 T', \quad (15a)$$

$$\bar{s}^2(m_Z^2) \approx 0.2334 + 0.0036 S - 0.0024 T' - 0.0026 \delta_\alpha, \quad (15b)$$

$$\bar{g}_W^2(0) \approx 0.4183 - 0.0030 S + 0.0044 T' + 0.0035 U + 0.0014 \delta_\alpha, \quad (15c)$$

where $T' = T + (0.0055 - \bar{\delta}_G)/\alpha$. The values of $\bar{g}_Z^2(m_Z^2)$ and $\bar{s}^2(0)$ are then calculated from $\bar{g}_Z^2(0)$ and $\bar{s}^2(m_Z^2)$ above, respectively, by assuming the SM running of the form-factors. The Z widths are sensitive to $\bar{g}_Z^2(m_Z^2)$, which can be obtained from $\bar{g}_Z^2(0)$ in the SM approximately by

$$\frac{1}{\bar{g}_Z^2(m_Z^2)} \approx \frac{1}{\bar{g}_Z^2(0)} - 0.02390 + \frac{2.41}{m_t^2} + \frac{1.73}{m_H^2} \quad (16)$$

when m_t (GeV) > 150 and m_H (GeV) > 100. Details of the following analysis will be reported elsewhere [67].

4.2. Global Fit to All the Electroweak Data

By assuming that all the vertex corrections except for the $Zb_L b_L$ vertex function $\bar{\delta}_b(m_Z^2)$ are dominated by the SM contributions, we make a four-parameter fit to the LEP/SLC data^a of Tables 1–3 in terms of $\bar{g}_Z^2(m_Z^2)$, $\bar{s}^2(m_Z^2)$, $\bar{\delta}_b(m_Z^2)$ and $\alpha_s = \alpha_s(m_Z)_{\overline{\text{MS}}}$. We find [67]

$$\left. \begin{aligned} \bar{g}_Z^2(m_Z^2) &= 0.55556 - 0.00049 \frac{\alpha'_s - 0.1081}{0.0043} \pm 0.00072 \\ \bar{s}^2(m_Z^2) &= 0.23041 + 0.00004 \frac{\alpha'_s - 0.1081}{0.0043} \pm 0.00029 \end{aligned} \right\} \rho_{\text{corr}} = 0.23, \quad (17a)$$

$$\chi_{\text{min}}^2 = 15.6 + \left(\frac{\alpha'_s - 0.1081}{0.0043} \right)^2 + \left(\frac{\bar{\delta}_b - 0.0025}{0.0042} \right)^2, \quad (17b)$$

where

$$\alpha'_s = \alpha_s(m_Z)_{\overline{\text{MS}}} + 1.54 \bar{\delta}_b(m_Z^2) \quad (18)$$

is the combination [5] that appears in the theoretical prediction for Γ_h . The best fit is obtained at $\bar{\delta}_b(m_Z^2) = 0.0025$ and $\alpha_s = 0.1043$ as a consequence of the R_b data: see Figs. 3 and 4. On the other hand, if we assume the SM value for $\bar{\delta}_b(m_Z^2)$, Eq.(5), the above fit gives $\alpha_s = 0.1234 \pm 0.0043$ for $m_t = 175$ GeV. In Fig. 7, we show the 1- σ (39%CL) allowed contours for $\alpha_s = 0.115, 0.120, 0.125$ when $\bar{\delta}_b$ takes its SM value at $m_t = 175$ GeV. If we allow *both* $\bar{\delta}_b(m_Z^2)$ and α_s to be freely fitted by the data, we obtain the solid contour in Fig. 7. The SM predictions for $\delta_\alpha = 0.03$ and their dependence on $\delta_\alpha - 0.03$ are also given. As expected, only $\bar{s}^2(m_Z^2)$ is sensitive to δ_α .

^aWe exclude from the fit the jet-charge asymmetry data in Table 1, since it allows an interpretation only within the minimal SM. It is included in our SM fit in section 5.

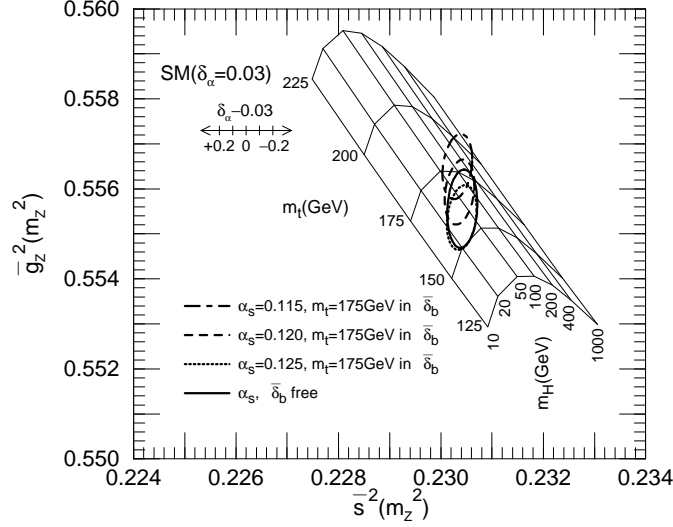


Fig. 7. A two-parameter fit to the Z boson parameters in the $(\bar{s}^2(m_Z^2), \bar{g}_Z^2(m_Z^2))$ plane, where $\alpha_s(m_Z)$ is treated as an external parameter and the $Zb_L b_L$ vertex form-factor, $\bar{\delta}_b(m_Z^2)$, is evaluated in the SM for $m_t = 175$ GeV. The $1-\sigma$ (39%CL) contours are shown for $\alpha_s = 0.115, 0.120$ and 0.125 . The solid contour is obtained by a four-parameter fit where both α_s and $\bar{\delta}_b(m_Z^2)$ are allowed to vary. Also shown are the SM predictions in the range $125 \text{ GeV} < m_t < 225 \text{ GeV}$ and $10 \text{ GeV} < m_H < 1000 \text{ GeV}$ at $\delta_\alpha \equiv 1/\bar{\alpha}(m_Z^2) - 128.72 = 0.03$ and their dependences on $\delta_\alpha - 0.03$.

The fit from the low-energy neutral-current data is updated [67] by including the new CCFR data [68]:

$$\left. \begin{aligned} \bar{g}_Z^2(0) &= 0.5441 \pm 0.0029 \\ \bar{s}^2(0) &= 0.2362 \pm 0.0044 \end{aligned} \right\} \quad \rho_{\text{corr}} = 0.70, \quad (19a)$$

$$\chi_{\text{min}}^2 = 2.7. \quad (19b)$$

More discussions on the role of the low-energy neutral-current experiments are given in the following subsection.

The W mass data in Table 1, $m_W = 80.26 \pm 0.16 \text{ GeV}$, gives

$$\bar{g}_W^2(0) = 0.4227 \pm 0.0017, \quad (20)$$

for $\bar{\delta}_G = 0.0055$.

We perform a five-parameter fit to all the electroweak data, the Z parameters, the W mass and the low-energy neutral-current data, in terms of $S, T, U, \bar{\delta}_b$ and α_s , where we set $m_t = 175 \text{ GeV}$ and $m_H = 100 \text{ GeV}$ in the mild running of the charge form-factors, e.g. in Eq.(16). We find

$$\left. \begin{aligned} S &= -0.42 - 0.059 \frac{\alpha'_s - 0.1093}{0.0042} + 0.06 \frac{\delta_\alpha - 0.03}{0.09} \pm 0.15 \\ T &= 0.57 - 0.104 \frac{\alpha'_s - 0.1093}{0.0042} \pm 0.17 \\ U &= 0.16 + 0.079 \frac{\alpha'_s - 0.1093}{0.0042} + 0.02 \frac{\delta_\alpha - 0.03}{0.09} \pm 0.49 \end{aligned} \right\} \quad \rho_{\text{corr}} = \begin{pmatrix} 1 & 0.86 & -0.10 \\ & 1 & -0.20 \\ & & 1 \end{pmatrix}, \quad (21a)$$

$$\chi_{\min}^2 = 20.4 + \left(\frac{\alpha'_s - 0.1093}{0.0042} \right)^2 + \left(\frac{\bar{\delta}_b - 0.0025}{0.0042} \right)^2. \quad (21b)$$

The dependence of the S and T parameters upon δ_α may be understood from Eq.(15). For an arbitrary value of $\bar{\delta}_G$ the parameter T should be replaced by $T' \equiv T + (0.0055 - \bar{\delta}_G)/\alpha$. It should be noted that the uncertainty in S coming from $\delta_\alpha = 0.03 \pm 0.09$ is of the same order as that from the uncertainty in α_s ; they are not negligible when compared to the overall error. The T parameter has little δ_α dependence, but it is sensitive to α_s .

The above results, together with the SM predictions, are shown in Fig. 8 as the projection onto the (S, T) plane. Accurate parametrizations of the SM contributions to the S, T, U parameters are found in Ref. [5]. Also shown are the predictions [7] of the minimal (one-doublet) $SU(N_c)$ Technicolor (TC) models with $N_c = 2, 3, 4$. It is clearly seen that the current experiments provide a fairly stringent constraint on the simple TC models if a QCD-like spectrum and the large N_c scaling are assumed [7]. It is necessary for a realistic TC model to provide an additional negative contribution to S [69] and a negligibly small contribution to T at the same time.

Finally, if we regard the point $(S, T, U) = (0, 0, 0)$ as the point with no-Electroweak corrections (a more precise treatment will be given in section 5.2), then we find $\chi_{\min}^2/(\text{d.o.f.}) = 141/(22)$ whose probability less than 10^{-18} . On the other hand, if we also switch-off the remaining electroweak corrections to G_F by setting $\bar{\delta}_G = 0$, then we find $T' = 0.0055/\alpha = 0.75$, and the point $(S, T', U) = (0, 0.75, 0)$ gives $\chi_{\min}^2/(\text{d.o.f.}) = 34.2/(22)$ which is consistent with the data at 5%CL. As emphasized in

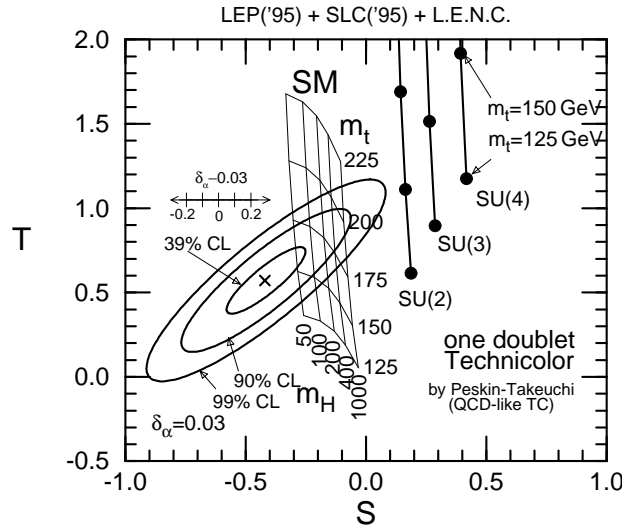


Fig. 8. Constraints on (S, T) from the five-parameter fit to all the electroweak data for $\delta_\alpha = 0.03$ and $\bar{\delta}_G = 0.0055$. Together with S and T , the U parameter, the $Zb_L b_L$ vertex form-factor, $\bar{\delta}_b(m_Z^2)$, and the QCD coupling, $\alpha_s(m_Z)$, are allowed to vary in the fit. Also shown are the SM predictions in the range $125 \text{ GeV} < m_t < 225 \text{ GeV}$ and $50 \text{ GeV} < m_H < 1000 \text{ GeV}$. The predictions [7] of one-doublet $SU(N_c)$ -TC models are shown for $N_c = 2, 3, 4$.

Ref. [70], the genuine electroweak correction is not trivial to establish in this analysis because of the cancellation between the large T parameter from $m_t \sim 175$ GeV and the non-universal correction $\bar{\delta}_G$ to the muon decay constant in the observable combination [5] $T' = T + (0.0055 - \bar{\delta}_G)/\alpha$.

4.3. Impact of the Low-Energy Neutral-Current Data

In this subsection, we show individual contributions from the four sectors of the low-energy neutral-current data [5], ν_μ - q and ν_μ - e processes, atomic parity violation (APV), and the classic e - D polarization asymmetry data.

The only new additional data this year is from the CCFR collaboration [68] which measured the ratio of the neutral-current and charged-current cross-sections in the ν_μ scattering off nuclei. By using the model-independent parameters of Ref. [71], they constrain the following linear combination,

$$K = 1.732g_L^2 + 1.119g_R^2 - 0.100\delta_L^2 - 0.086\delta_R^2, \quad (22)$$

and find

$$K = 0.5626 \pm 0.0025 (\text{stat}) \pm 0.0036 (\text{sys}) \pm 0.0028 (\text{model}) \pm 0.0029 (m_c). \quad (23)$$

Because of the significantly high $\langle Q^2 \rangle_{\text{CCFR}} = 36 \text{ GeV}^2$ of the CCFR experiments as compared to the average of the old data [71] ($\langle Q^2 \rangle_{\text{HF}} = 20 \text{ GeV}^2$), the q^2 -dependent electroweak corrections are different, and we cannot combine the two data sets within the model-independent framework.

By noting that the data were obtained after correcting for the external photonic corrections we find [67] from the CCFR data (23)

$$\bar{s}^2(0) = 0.2421 + 1.987[\bar{g}_Z^2(0) - 0.5486] \pm 0.0058. \quad (24)$$

The corresponding fit to the old data [71] gives^b

$$\left. \begin{aligned} \bar{g}_Z^2(0) &= 0.5454_{-0.0082}^{+0.0076} \\ \bar{s}^2(0) &= 0.2419_{-0.0142}^{+0.0130} \end{aligned} \right\} \quad \rho_{\text{corr}} = 0.916, \quad (25a)$$

$$\chi_{\text{min}}^2 = 0.13. \quad (25b)$$

By combining with all the other neutral-current data of Ref. [5] we find the fit Eq.(19). In order to compare these constraints with those from the LEP/SLC experiments it is useful to re-express the fit in the $(\bar{s}^2(m_Z^2), \bar{g}_Z^2(m_Z^2))$ plane by assuming the SM running of the charge form-factors. The combined fit of Eq.(19) then becomes

$$\left. \begin{aligned} \bar{g}_Z^2(m_Z^2) &= 0.5512 \pm 0.0030 \\ \bar{s}^2(m_Z^2) &= 0.2277 \pm 0.0047 \end{aligned} \right\} \quad \rho_{\text{corr}} = 0.70, \quad (26a)$$

$$\chi_{\text{min}}^2 = 2.7. \quad (26b)$$

^bThe data in Ref. [71] were also corrected for the external photonic corrections. The $\delta_{c.c.}$ correction in Ref. [5] was hence double counting. The fit Eq.(4.17) of Ref. [5] has been revised here.

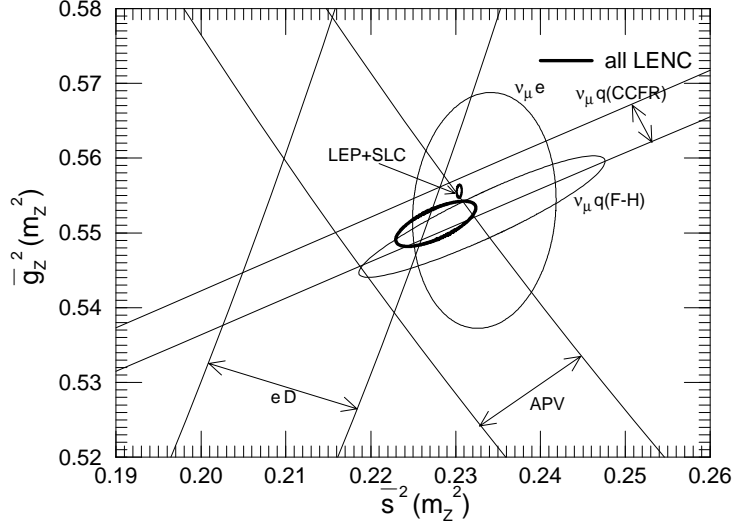


Fig. 9. Fit to the low-energy neutral-current data in terms of the two universal charge form-factors $\bar{s}^2(m_Z^2)$ and $\bar{g}_Z^2(m_Z^2)$. 1- σ (39%CL) contours are shown separately for the old [71] and the new [68] ν_μ - q data, the ν_μ - e data, the atomic parity violation (APV) data, and the SLAC e -D polarization asymmetry data. The 1- σ contour of the combined fit, Eq.(26), is shown by the thick contour. Also shown is the constraint from the LEP/SLC data, which is the solid contour in Fig. 7.

In Fig. 9 we show individual contributions to the fit, together with the combined LEP/SLC fit (the solid contour of Fig. 7). It is clear that the low-energy data have little impact on constraining the effective charges, or equivalently the S and T parameters. They constrain, however, possible new interactions beyond the $SU(2)_L \times U(1)_Y$ gauge interactions, such as those from an additional Z boson [72]. The model-independent parametrization of the low-energy data is hence highly desirable.

5. The Minimal Standard Model Confronts the Electroweak Data

In this section we assume that all the radiative corrections are dominated by the SM contributions and obtain constraints on m_t and m_H from the electroweak data.

5.1. Constraints on m_t and m_H as Functions of α_s and $\bar{\alpha}(m_Z^2)$

In the minimal SM all the form-factors, $\bar{g}_Z^2(m_Z^2)$, $\bar{s}^2(m_Z^2)$, $\bar{g}_Z^2(0)$, $\bar{s}^2(0)$, $\bar{g}_W^2(0)$ and $\bar{\delta}_b(m_Z^2)$, depend uniquely on the two mass parameters m_t and m_H . Fig. 10 shows the result of the global fit to all electroweak data in the (m_H, m_t) plane for (a) $\alpha_s = 0.115$ and (b) 0.120 with $\delta_\alpha = 0.03$, and with (c) $\delta_\alpha = -0.06$ and (d) +0.12 for $\alpha_s = 0.120$. The thick inner and outer contours correspond to $\Delta\chi^2 \equiv \chi^2 - \chi_{\min}^2 = 1$ (39%CL), and $\Delta\chi^2 = 4.61$ (90%CL), respectively. The minimum of χ^2 is indicated by an “ \times ” and the corresponding values of χ_{\min}^2 are given. We also give the separate 1- σ constraints arising from the Z -pole asymmetries, Γ_Z , and m_W . The asymmetries

constrain m_t and m_H through $\bar{s}^2(m_Z^2)$, while Γ_Z constrains them through the three form-factors $\bar{g}_Z^2(m_Z^2)$, $\bar{s}^2(m_Z^2)$ and $\bar{\delta}_b(m_Z^2)$. In other words, the asymmetries measure the combination of S and T as in Eq.(15b); both S and T are functions of m_t and m_H [5]. On the other hand, Γ_Z measures a different combination of S and T with an additional constraint from $\bar{\delta}_b$. A remarkable point apparent from Fig. 10 is that, in the SM, when m_t and m_H are much larger than m_Z , Γ_Z depends upon almost the same combination of m_t and m_H as the one measured through $\bar{s}^2(m_Z^2)$. This is because the quadratic m_t -dependence of $\bar{g}_Z^2(m_Z^2)$ and that of $\bar{\delta}_b$ largely cancel in the

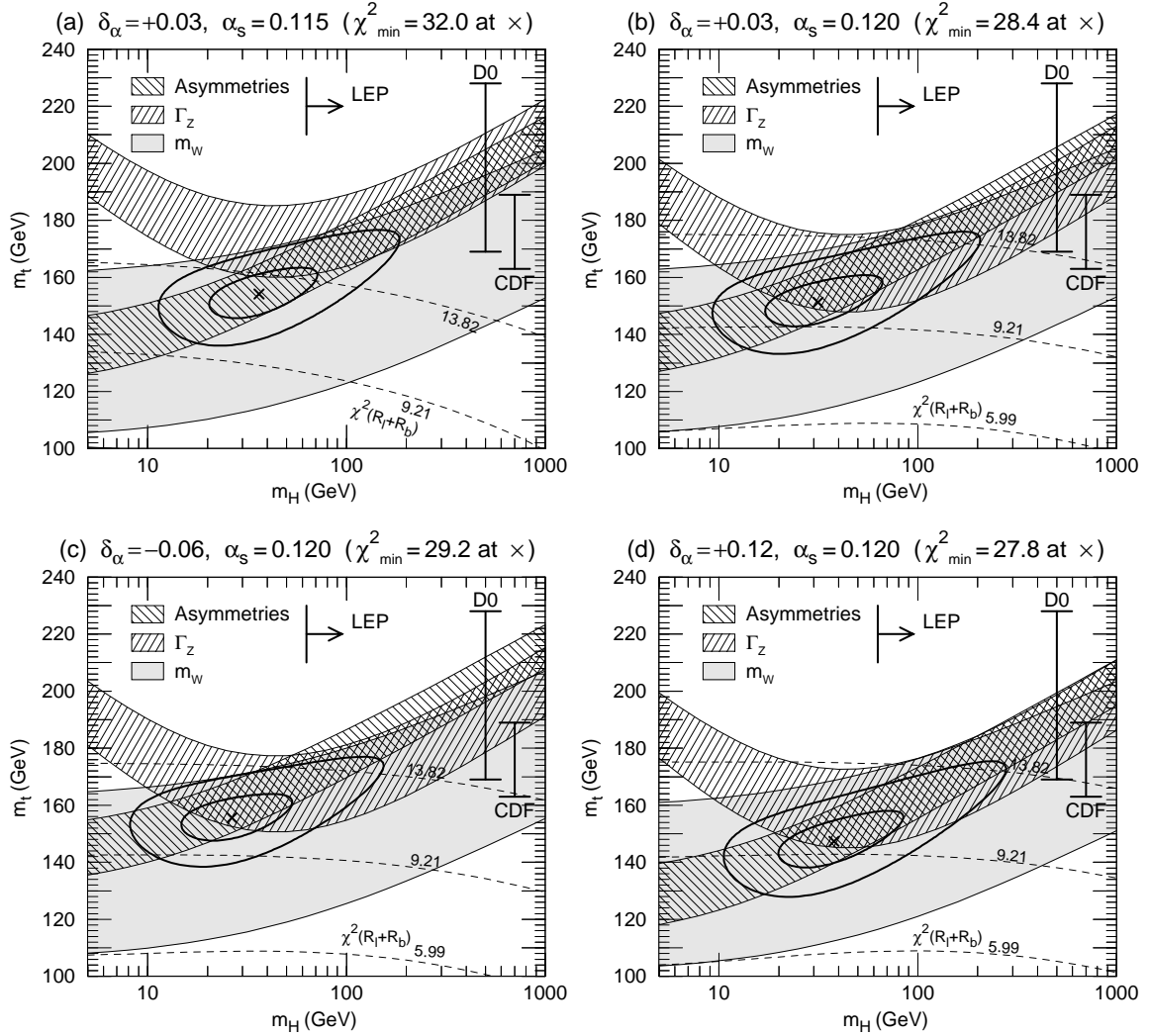


Fig. 10. The SM fit to all electroweak data in the (m_H, m_t) plane for $(\delta_\alpha, \alpha_s) = (+0.03, 0.115)$ (a), $(+0.03, 0.120)$ (b), $(-0.06, 0.120)$ (c) and $(+0.12, 0.120)$ (d), where $\delta_\alpha = 1/\bar{\alpha}(m_Z^2) - 128.72$ [5]. The thick inner and outer contours correspond to $\Delta\chi^2 = 1$ ($\sim 39\%$ CL), and $\Delta\chi^2 = 4.61$ ($\sim 90\%$ CL), respectively. The minimum of χ^2 is marked by an “x”. Also shown are the $1\text{-}\sigma$ constraints from the Z -pole asymmetries, Γ_Z and m_W . The dashed lines show the constraint only from R_ℓ and R_b . The contours for $\chi^2 = 5.99, 9.21, 13.82$ correspond to 95%, 99% and 99.9%CL boundaries, respectively.

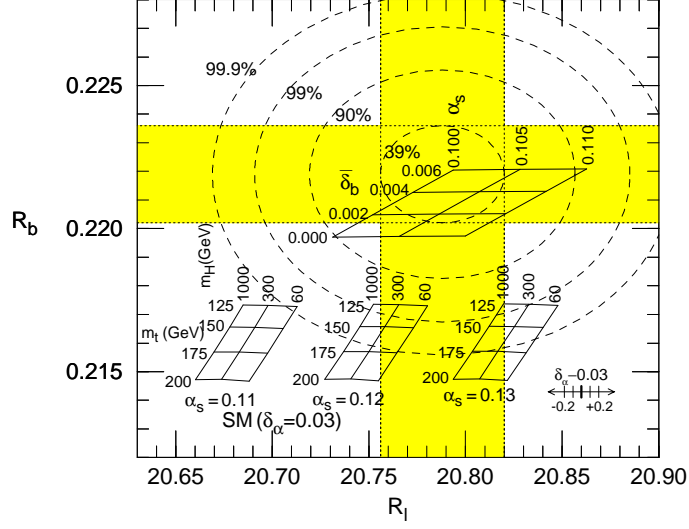


Fig. 11. The R_b vs R_ℓ plane. The SM predictions are shown in the range $120 \text{ GeV} < m_t < 240 \text{ GeV}$, and $60 \text{ GeV} < m_H < 1 \text{ TeV}$, for three cases of α_s ($\alpha_s = 0.11, 0.12$ and 0.13). These predictions are for $\delta_\alpha = 0.03$, and their dependences on δ_α are also indicated. Also shown are the 39%, 90%, 99% and 99.9% CL contours obtained by combining only the R_ℓ and R_b data. The $(\alpha_s, \bar{\delta}_b)$ lattice is obtained by allowing $\bar{\delta}_b$ to vary at $\bar{s}^2(m_Z^2) = 0.23039$ from Eq.(3).

SM prediction for Γ_Z . Because of this only a band of m_t and m_H can be strongly constrained from the asymmetries and Γ_Z alone despite their very small experimental errors. The constraint from the m_W data overlaps this allowed region.

Quantities which help to disentangle the above m_t - m_H correlation are R_ℓ and R_b . The constraints from these data are shown in Fig. 10 by dashed lines corresponding to $\chi^2 = 5.99$ (95%CL), $\chi^2 = 9.21$ (99%CL) and $\chi^2 = 13.82$ (99.9%CL) contours. These constraints can be clearly seen in Fig. 11 where we show the data and the SM predictions for R_ℓ and R_b . R_ℓ is sensitive to the assumed value of α_s , and, for $\alpha_s = 0.120$, the data favors smaller m_H . R_b is, on the other hand, sensitive to neither α_s nor m_H , and the data strongly disfavors large m_t . It is thus the R_ℓ and R_b data that constrain the values of m_t and m_H from above. If it were not for the data on R_ℓ and R_b the common shaded region in Fig. 10 with very large m_H ($m_H \sim 1 \text{ TeV}$) could not be excluded by the electroweak data alone.

It is clearly seen from Fig. 10 that the narrow “asymmetry” band is sensitive to δ_α , whereas the “ Γ_Z ” constraint is sensitive to α_s . The fit improves at larger δ_α (larger $1/\bar{\alpha}(m_Z^2)$) because the “asymmetry” constraint then favors lower m_t that is favored by the R_b data.

The χ^2 function of the global fit to all electroweak data can be parametrized in terms of the four parameters m_t , m_H , α_s and δ_α :

$$\chi_{\text{SM}}^2(m_t, m_H, \alpha_s, \delta_\alpha) = \left(\frac{m_t - \langle m_t \rangle}{\Delta m_t} \right)^2 + \chi_H^2(m_H, \alpha_s, \delta_\alpha), \quad (27a)$$

with

$$\langle m_t \rangle = 163.3 + 13.1 \ln \frac{m_H}{100} + 0.8 \ln^2 \frac{m_H}{100} - 3.1 \left(\frac{\alpha_s - 0.12}{0.01} \right) - 4.9 \left(\frac{\delta_\alpha - 0.03}{0.09} \right), \quad (27b)$$

$$\Delta m_t = 6.7 - 0.07 \ln \frac{m_H}{100} - \left(0.018 - 0.003 \ln \frac{m_H}{100} \right) \frac{m_t - 175}{10}, \quad (27c)$$

and

$$\begin{aligned} \chi_H^2(m_H, \alpha_s, \delta_\alpha) = & 27.0 + \left(\frac{\delta_\alpha - 0.44}{0.23} \right)^2 + \left(\frac{\alpha_s - 0.1222 + 0.0014 \delta_\alpha}{0.0036} \right)^2 \\ & - \left(\frac{\alpha_s - 0.1470 + 0.052 \delta_\alpha}{0.0087} \right) \ln \frac{m_H}{100} - \left(\frac{\alpha_s - 0.1315}{0.0174} \right) \ln^2 \frac{m_H}{100}. \end{aligned} \quad (27d)$$

Here m_t and m_H are measured in GeV. This parametrization reproduces the exact χ^2 function within a few percent accuracy in the range $100 \text{ GeV} < m_t < 250 \text{ GeV}$, $60 \text{ GeV} < m_H < 1000 \text{ GeV}$ and $0.10 < \alpha_s(m_Z) < 0.13$. The best-fit value of m_t for a given set of m_H , α_s and δ_α is readily obtained from Eq.(27b) with its approximate error of (27c).

For $m_H = 60, 300, 1000 \text{ GeV}$, $\alpha_s = 0.120 \pm 0.07$ and $\delta_\alpha = 0.03 \pm 0.09$, one obtains

$$m_t = 179 \pm 7_{-22(m_H=60)}^{+19(m_H=1000)} \mp 2(\alpha_s) \mp 5(\delta_\alpha), \quad (28)$$

where the mean value is for $m_H = 300 \text{ GeV}$. The fit (28) agrees excellently with the estimate [73]

$$m_t = 180 \pm 13 \text{ GeV} \quad (29)$$

from the direct production data at Tevatron [8, 9]. Despite the claim [70] that there is no strong evidence for the genuine electroweak correction, which we re-confirmed in the previous section with the new data, I believe that this is a strong evidence that the standard electroweak gauge theory is valid at the quantum level. The accidental cancellation of the two large radiative effects in the observable combination $T' = T + (0.0055 - \bar{\delta}_G)/\alpha$ should give us, in the face of the Tevatron results (29), a strong evidence for the presence of the electroweak correction to the muon decay, $\bar{\delta}_G$, which is finite and calculable only in the gauge theory [74].

Due to the quadratic form of Eq.(27) it is easy to obtain results which are independent of α_s and/or δ_α . Also, additional constraints on the external parameters α_s and δ_α , such as those from their improved measurements or the constraint from the grand unification of these couplings may be added without difficulty. Here we give a parametrization of the constraint on $\alpha_s \equiv \alpha_s(m_Z)_{\overline{\text{MS}}}$ from the electroweak data within the minimal SM:

$$\alpha_s = 0.1282 \pm 0.0035 - 0.0105 \left(\frac{m_t}{175} \right)^2 + 0.00045 \ln^2 \frac{m_H}{7.8} - 0.0008 \frac{\delta_\alpha - 0.03}{0.09}, \quad (30)$$

Table 5. 95%CL upper and lower bounds of m_H (GeV) for a given α_s and $\delta_\alpha = 0.03 \pm 0.09$ [3]

α_s	all EW data	$-(R_b, R_c)$ data	$+m_t$ (Tevatron)
0.115	$16 < m_H < 150$	$18 < m_H < 290$	$22 < m_H < 360$
0.120	$13 < m_H < 180$	$15 < m_H < 500$	$20 < m_H < 550$
0.125	$11 < m_H < 220$	$12 < m_H < 1800$	$18 < m_H < 980$

which reproduces the results (see Fig. 4) well in the range $150 < m_t$ (GeV) < 200, $60 < m_H$ (GeV) < 1000 and $|\delta_\alpha| < 0.2$.

As discussed above, the constraint on m_H from the electroweak data is sensitive to the R_b , and hence on α_s . Shown in Table 5 are the 95%CL upper and lower bounds on m_H (GeV) from the electroweak data. Low mass Higgs boson is clearly favored. However, this trend disappears for $\alpha_s > 0.12$ once we remove the R_b and R_c data. The present m_t estimate (29) from Tevatron does not significantly improve the situation.

It is instructive to anticipate the impact a precise measurement of the top-quark mass would have in the context of the present electroweak data. For instance, precision measurement of m_t with an error of 1 GeV is envisaged at TeV33 [75], a proposed luminosity upgrade of Tevatron. In the discussion below we treat m_t as an external parameter, and hence we discuss the sensitivity of the present electroweak data to m_H while assuming that m_t is known precisely.

The 95%CL upper/lower bounds on m_H from the electroweak data are shown in Fig. 12 as functions of m_t . Dependences of the bounds on the two remaining parameters, $\alpha_s = \alpha_s(m_Z)_{\overline{\text{MS}}}$ and $\delta_\alpha = 1/\bar{\alpha}(m_Z^2) - 128.72$, are shown clearly. For

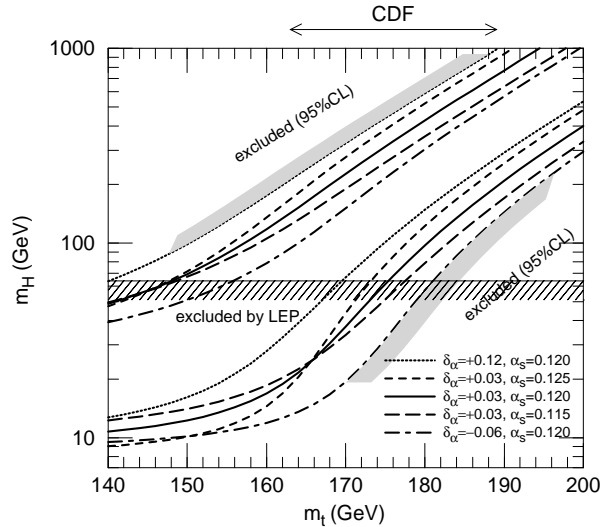


Fig. 12. Constraints on the Higgs mass in the SM from all the electroweak data. Upper and lower bounds of the Higgs mass at 95% CL are shown as functions of the top mass m_t , where m_t is treated as an external parameter with negligible uncertainty. The results are shown for $\alpha_s = 0.120 \pm 0.005$ and $\delta_\alpha \equiv 1/\bar{\alpha}(m_Z^2) - 128.72 = 0.03 \pm 0.09$.

a smaller value of m_t , $m_t < 170$ GeV, a rather stringent upper bound on m_H is obtained, whereas medium heavy Higgs boson is favored for $m_t > 180$ GeV. It is tantalizing that the present data from Tevatron (29) lies just on the boundary.

Fig. 12 shows us that once the top-quark mass is determined, either by direct measurements or by a theoretical model, the major remaining uncertainty is in δ_α , the magnitude of the QED running coupling constant at the m_Z scale. It is clear that we won't be able to learn about m_H in the SM, nor about physics beyond the SM from its quantum effects, without a significantly improved determination of $\bar{\alpha}(m_Z^2)$.

Shown in Fig. 13 is the relative contributions to the uncertainty in the present determination of $\Delta\alpha(m_Z^2)$ based on the dispersion integral over the $\sigma(e^+e^- \rightarrow \text{hadrons})$ data, taken from Ref. [58]. It is clearly seen that the majority of the uncertainty comes from the low energy region, $\sqrt{s} < 5$ GeV. The ϕ factory DAΦNE and upgraded VEPP-2M will be able to improve our knowledge at $\sqrt{s} \lesssim 1.5$ GeV. However, by far the largest uncertainty comes from the region $\sqrt{s} = 2.5\text{--}5.0$ GeV which a future τ -charm factory can cover. Precision measurements of the τ hadronic decay rates will further give us normalization of the e^+e^- hadro-production cross section upon use of the CVC (Conserved Vector Current) rule of QCD [76]. I believe that a τ -charm factory, if realised in the near future, will contribute most efficiently toward

range (\sqrt{s})	possible improvements in the future
ρ	$\left. \begin{array}{l} \text{DA}\Phi\text{NE} \\ \text{VEPP-2M} \end{array} \right\} \left. \begin{array}{l} \tau\text{-charm \& B factories} \\ (\text{hadronic } \tau\text{-decays} + \text{CVC}) \end{array} \right\}$
1.05–2.5 GeV	
narrow resonances	$\left. \begin{array}{l} \\ \\ \end{array} \right\} \tau\text{-charm factory}$
2.5–5 GeV	
5–7 GeV	
7–12 GeV	$\left. \begin{array}{l} \\ \end{array} \right\} \text{B factory}$
>12 GeV	

Fig. 13. Relative contributions to the uncertainty in $\Delta\alpha_{\text{had}}(m_Z^2)$ by Burkhardt and Pietrzyk [58]. Possible improvements from the future generation experiments are indicated.

sharpening of $\bar{\alpha}(m_Z^2)$.

5.2. Is there already indirect evidence for the standard W self-coupling?

The success of the SM predictions against precision electroweak experiments at the quantum level suggests a question if there is already evidence for the standard universal gauge-boson self-couplings. It is not trivial to answer this question definitely since we should identify which finite portion of the quantum corrections is sensitive to the weak-boson self-interactions. Usually one splits the complete SM radiative corrections into just two pieces which are separately gauge invariant, the fermionic loop contributions to the gauge-boson self-energies, and the rest. It can then be stated clearly that neither of the corrections alone is consistent with the data, and both contributions are needed to explain the success of the SM radiative corrections [74]. Since the bosonic part of the correction should necessarily contain the weak boson self-interactions, we may already have evidence for universal couplings.

It is not clear to me, however, how much of these finite bosonic correction terms depend on the splitting of the gauge bosons into themselves. For instance, the box diagrams do not contain gauge-boson self-couplings. I therefore split the bosonic corrections into three separately gauge-invariant pieces, ‘box-like’, ‘vertex-like’ and ‘propagator-like’ pieces by appealing to the S-matrix pinch technique [51]. It is then only the ‘vertex-like’ and ‘propagator-like’ pieces which contain the gauge boson self-couplings. Schematically we separate the SM radiative corrections into the following five pieces:

$$\begin{aligned}
\mathcal{M} &= \text{QED/QCD} & (A) \\
&+ \text{fermion-loop} \quad \text{---}\bigcirc\text{---} & (B) \\
&+ \text{box} \quad \text{---}\text{---}\text{---}\text{---} & (C) \\
&+ \text{vertex} \quad \text{---}\text{---}\text{---} + \text{---}\text{---}\text{---} & (D) \\
&+ \text{bosonic-loop} \quad \text{---}\text{---}\text{---} + \text{---}\text{---}\text{---} + \text{---}\text{---}\text{---} & (E)
\end{aligned} \tag{31}$$

Details of this separation for each radiative correction term may be obtained straightforwardly from the analytic expressions presented in Ref. [5]. We find by confronting these ‘predictions’ with the latest electroweak data the results of Table 6.

The ‘no-EW’ entry confronts the tree-level predictions of the SM where only QCD and external QED corrections are applied. In this column $\bar{\alpha}(m_Z^2)$ is calculated by including only contributions from light quarks and leptons with $\delta_h = 0.03$ [5] for the hadronic uncertainty. It is quite striking to re-confirm the observation [70] that these ‘no-EW’ predictions agree with experiments at LEP/SLC very well. In fact, it gives even better χ^2 than the SM, partly because of the R_b data, which prefers no electroweak corrections $\bar{\delta}_b(m_Z^2) = 0$ over the SM prediction $\bar{\delta}_b(m_Z^2) = -0.0099$ for

Table 6. The electroweak data and the SM predictions. The three predictions for Γ_Z , σ_h^0 and R_ℓ are for $\alpha_s = 0.115, 0.120$ and 0.125 .

	data	no-EW	+fermion	+box	+vertex	+propagator		
m_t (GeV)		—	175	175	175	175	175	175
m_H (GeV)		—	100	—	100	60	300	1000
S		—	-0.066	-0.066	-0.066	-0.283	-0.146	-0.075
T		—	1.134	1.134	1.134	0.908	0.759	0.578
U		—	0.014	0.014	0.014	0.357	0.352	0.351
δ_G		—	—	0.00429	0.00549	0.00549	0.00549	0.00549
$1/\bar{\alpha}(m_Z^2)$		128.89	128.90	128.90	128.90	128.75	128.75	128.75
$\bar{s}^2(m_Z^2)$		0.23112	0.22814	0.22954	0.22994	0.23008	0.23093	0.23162
$\bar{g}_Z^2(m_Z^2)$		0.54865	0.55813	0.55571	0.55504	0.55642	0.55594	0.55520
$\bar{\delta}_b(m_Z^2)$		—	—	—	-0.00993	-0.00995	-0.00991	-0.00997
$\bar{s}^2(0)$		0.23865	0.23583	0.23715	0.23752	0.23850	0.23930	0.23995
$\bar{g}_Z^2(0)$		0.54865	0.55323	0.55085	0.55019	0.54928	0.54868	0.54796
$\bar{g}_W^2(0)$		0.42185	0.42714	0.42453	0.42380	0.42448	0.42338	0.42236
Γ_Z (GeV)	2.4963 ± 0.0032	2.4838 2.4866 2.4894	2.5348 2.5377 2.5405	2.5200 2.5229 2.5257	2.4907 2.4935 2.4963	2.4965 2.4994 2.5022	2.4922 2.4950 2.4978	2.4870 2.4898 2.4926
σ_h^0 (nb)	41.488 ± 0.078	41.505 41.478 41.452	41.498 41.471 41.445	41.500 41.474 41.447	41.487 41.460 41.434	41.487 41.461 41.434	41.490 41.464 41.437	41.494 41.468 41.441
R_ℓ	20.788 ± 0.032	20.768 20.802 20.835	20.817 20.851 20.884	20.795 20.828 20.862	20.734 20.767 20.801	20.731 20.765 20.798	20.716 20.750 20.784	20.703 20.737 20.770
$A_{\text{FB}}^{0,\ell}$	0.0172 ± 0.0012	0.0169	0.0224	0.0198	0.0175	0.0172	0.0157	0.0145
A_τ	0.1418 ± 0.0075	0.1502	0.1733	0.1625	0.1517	0.1506	0.1439	0.1384
A_e	0.1390 ± 0.0089	0.1502	0.1733	0.1625	0.1517	0.1506	0.1439	0.1384
R_b	0.2219 ± 0.0017	0.2182	0.2181	0.2182	0.2157	0.2157	0.2157	0.2157
R_c	0.1540 ± 0.0074	0.1717	0.1719	0.1718	0.1722	0.1722	0.1721	0.1721
$A_{\text{FB}}^{0,b}$	0.0997 ± 0.0031	0.1054	0.1219	0.1142	0.1063	0.1056	0.1008	0.0968
$A_{\text{FB}}^{0,c}$	0.0729 ± 0.0058	0.0753	0.0882	0.0822	0.0763	0.0757	0.0720	0.0690
$\sin^2 \theta_{eff}^{lept} (\langle Q_{\text{FB}} \rangle)$	0.2325 ± 0.0013	0.2311	0.2282	0.2296	0.2309	0.2311	0.2319	0.2326
A_{LR}	0.1551 ± 0.0040	0.1502	0.1733	0.1625	0.1517	0.1506	0.1439	0.1384
$A_b(\text{LR})$	0.841 ± 0.053	0.936	0.938	0.937	0.935	0.935	0.934	0.934
$A_c(\text{LR})$	0.606 ± 0.090	0.669	0.679	0.674	0.670	0.669	0.666	0.664
χ^2	$(\alpha_s = 0.115)$	35.0	296.4	117.2	34.5	30.2	34.4	57.1
	$(\alpha_s = 0.120)$	28.7	320.3	131.8	29.6	28.2	29.3	48.4
	$(\alpha_s = 0.125)$	26.6	348.3	150.5	28.8	30.4	28.3	43.9
g_L^2	0.2980 ± 0.0044	0.2955	0.3027	0.3049	0.3067	0.3049	0.3037	0.3024
g_R^2	0.0307 ± 0.0047	0.0309	0.0307	0.0307	0.0298	0.0300	0.0301	0.0302
δ_L^2	-0.0589 ± 0.0237	-0.0601	-0.0606	-0.0652	-0.0645	-0.0645	-0.0645	-0.0645
δ_R^2	0.0206 ± 0.0160	0.0186	0.0184	0.0184	0.0179	0.0180	0.0180	0.0181
χ^2		0.4	1.8	4.0	5.5	3.6	2.4	1.5
K (CCFR)	0.5626 ± 0.0060	0.5519	0.5641	0.5685	0.5703	0.5674	0.5653	0.5632
χ^2		3.2	0.1	1.0	1.6	0.6	0.2	0.0
s_{eff}^2	0.233 ± 0.008	0.239	0.236	0.235	0.229	0.230	0.231	0.231
ρ_{eff}	1.007 ± 0.028	1.000	1.008	1.016	1.015	1.013	1.012	1.011
χ^2		0.6	0.1	0.1	0.4	0.2	0.1	0.1
Q_W	-71.04 ± 1.81	-74.73	-74.73	-72.96	-72.91	-73.00	-73.10	-73.14
χ^2		4.2	4.2	1.1	1.1	1.2	1.3	1.3
$2C_{1u} - C_{1d}$	0.938 ± 0.264	0.709	0.725	0.730	0.729	0.724	0.721	0.718
$2C_{2u} - C_{2d}$	-0.659 ± 1.228	0.082	0.100	0.103	0.112	0.106	0.101	0.097
χ^2		1.9	1.2	1.1	1.1	1.2	1.4	1.5
m_W	80.26 ± 0.16	79.96	80.46	80.38	80.36	80.43	80.32	80.23
χ^2		3.5	1.6	0.6	0.4	1.1	0.2	0.0
χ_{tot}^2	$(\alpha_s = 0.115)$	48.8	305.3	125.0	44.6	38.1	40.0	61.6
	$(\alpha_s = 0.120)$	42.5	329.2	139.6	39.7	36.1	34.9	52.9
	$(\alpha_s = 0.125)$	40.4	357.2	158.4	38.9	38.3	33.9	48.3

$m_t = 175$ GeV. It is only the m_W value [77] and the atomic parity violation data

which give significantly higher χ^2 than the SM does.

The next ‘+fermion’ column^c gives the result of $A + B$ in Eq.(31). That the LEP/SLC data can be fitted well by the ‘no-EW’ calculation is a consequence of an accidental cancellation between the vertex/box correction to the μ decay matrix elements (the factor $\bar{\delta}_G$ in the Table) and the T parameter for $m_t \sim 175$ GeV in the observable combination $T' \equiv T + (0.0055 - \bar{\delta}_G)/\alpha$. If we include only the fermionic corrections the T parameter grows from zero to 1.144, while the factor $\bar{\delta}_G$ remains zero [5]. The jump of χ^2 from 30 to 300 in the LEP/SLC experiments is a consequence of the absence of this cancellation in T' .

It turned out that the ‘box-like’ corrections to the μ -decay matrix elements give almost 80% of the total $\bar{\delta}_G$ value. Hence by adding the ‘box-like’ corrections, the fit improves significantly. This can be seen from the column of ‘+box’, where we give results of A+B+C corrections in Eq.(31).

Up to this stage no contribution from quantum fluctuations with the weak-boson self-couplings are counted. It is in the next step, the ‘+vertex’ column where I list the results of A+B+C+D corrections, we can start to see their effects. It turns out that the effects of the remaining 20% correction to $\bar{\delta}_G$ and the effects in part from the vertex corrections in the Z -decay matrix elements significantly reduce the χ^2 in the LEP/SLC sector of the experiments from about 130 down to 30.

I should therefore conclude that the effect of the ‘vertex-like’ corrections is significant for the success of the SM at the quantum correction level. Even setting aside the fundamental problem that we could not control quantum fluctuations at short distances if it were not for the universality of the weak-boson self-couplings, it is reassuring to learn that, after cancellation of the short-distance singularity, the remaining finite correction makes the fit even better. I note in passing that the significance of the ‘propagator-like’ correction term which contains the Higgs-mass dependence of the SM prediction cannot be established at the present level of accuracy.

6. Conclusions

(i) The precision electroweak experiments at LEP and SLC test the SM predictions at a few times 10^{-3} level, which is sufficient to resolve some of the radiative effects.

(ii) All the data agree well with the predictions of the SM except for R_b and R_c measured at LEP, which gives 3% larger R_b at $3.7\text{-}\sigma$ and 11% smaller R_c at $2.5\text{-}\sigma$. When combined the two data alone would rule out the SM at 99.99%CL for $m_t > 170$ GeV.

(iii) If we allow only Γ_b and Γ_c to deviate from the SM predictions, then the data on R_b and R_c implies un-acceptably large α_s .

(iv) If we assume the SM value for Γ_c , then the R_b data is still 2% larger than the

^c $m_H = 100$ GeV is chosen to fix the negligible two-loop contributions in the ‘+fermion’ and ‘+vertex’ columns.

SM prediction at $3\text{-}\sigma$. Several theoretical models have been proposed to explain the discrepancy. The common consequence of allowing only Γ_b to deviate from the SM is small α_s , $\alpha_s = 0.104 \pm 0.008$.

(v) If we allow the QCD coupling α_s to vary in the global fit to the electroweak data, the R_b problem does not affect the standard S , T , U analysis. The (S, T) fit agrees excellently with the SM, but disfavors the naive QCD-like technicolor models.

(vi) The global fit in the minimal SM constrains (m_t, m_H) , where the preferred m_t range agrees well with the top-quark data at Tevatron.

(vii) Once m_t is known precisely, an improved constraint on m_H from precision electroweak experiments will be achieved only with the improved measurement on $\Delta\alpha_{\text{had}}(m_Z^2)$. The contribution of a future τ -charm factory will be decisive.

(viii) The agreement of the SM predictions with precision experiments improves significantly when one includes radiative effects due to ‘vertex-like’ corrections which may be regarded as indirect evidence for the universal weak-boson self-couplings.

7. Acknowledgements

I would like to thank D. Haidt, N. Kitazawa, S. Matsumoto and Y. Yamada for fruitful collaborations which made this presentation possible. I would also like to thank S. Aoki, B. Bullock, D. Charlton, M. Drees, S. Erredi, G.L. Fogli, R. Jones, J. Kanzaki, C. Mariotti, A.D. Martin, K. McFarland, T. Mori, M. Morii, D.R.O. Morrison, B. Pietrzyk, P.B. Renton, M.H. Shaevitz, D. Schaile, M. Swartz, R. Szalapski, T. Takeuchi, P. Vogel, P. Wells and D. Zeppenfeld for discussions that helped me understand the experimental data and their theoretical implications better.

8. References

- [1] The LEP Electroweak Working Group, Internal Note LEPEWWG/95-02 (CERN, 1 Aug. 1995).
- [2] The LEP Electroweak Heavy Flavours Working Group, Internal Note LEPHF/95-02 (CERN, 25 Jul. 1995).
- [3] S. Eidelman and F. Jegerlehner, *Z. Phys.* **C67** (1995) 602.
- [4] P.B. Renton, in these proceedings.
- [5] K. Hagiwara, D. Haidt, C.S. Kim and S. Matsumoto, *Z. Phys.* **C64** (1994) 559; **C68** (1995) 352(E); S. Matsumoto, *Mod. Phys. Lett.* **A10** (1995) 2553.
- [6] S. Bethke, Talk presented at the *XXX'th Rencontre de Moriond*, Les Arcs, France, March 19–26, 1995.
- [7] M.E. Peskin and T. Takeuchi, *Phys. Rev. Lett.* **65** (1990) 964; *Phys. Rev.* **D46** (1992) 381.
- [8] CDF Collaboration, F. Abe *et al.*, *Phys. Rev. Lett.* **74** (1995) 2626.
- [9] D0 Collaboration, S. Abachi *et al.*, *Phys. Rev. Lett.* **74** (1995) 2632.

- [10] M. Shifman, *Mod. Phys. Lett.* **A10** (1995) 605.
- [11] Particle Data Group, L. Montanet *et al.*, *Phys. Rev.* **D50** (1994) 1173.
- [12] D. Harris, CCFR collab., Talk presented at the *XXX'th Rencontre de Moriond*, Les Arcs, France, March 19–26, 1995.
- [13] A.X. El-Khadra *et al.*, *Phys. Rev. Lett.* **69** (1992) 729.
- [14] C.T.H. Davies *et al.*, *Phys. Rev.* **D50** (1994) 6963; *Phys. Lett.* **B345** (1995) 42.
- [15] K. Baird, SLD collab., Talk presented at the *XXX'th Rencontre de Moriond*, Les Arcs, France, March 19–26, 1995.
- [16] T. Truong, *Phys. Rev.* **D47** (1993) 3999.
- [17] G. Altarelli, P. Nason and G. Ridolfi, *Z. Phys.* **C68** (1995) 257.
- [18] G. Buchalla, I. Dunietz and H. Yamamoto, Preprint FERMILAB-PUB-95-167-T, hep-ph/9507437.
- [19] M. Neubert, in these proceedings.
- [20] M. Boulware and D. Finnell, *Phys. Rev.* **D44** (1991) 2054.
- [21] G. Altarelli, R. Barbieri and F. Caravaglios, *Phys. Lett.* **B314** (1993) 357.
- [22] J.D. Wells, C. Kolda and G.L. Kane, *Phys. Lett.* **B338** (1994) 219.
- [23] J.E. Kim and G.T. Park, *Phys. Rev.* **D50** (1994) 6686; **D51** (1995) 2444.
- [24] D. Garcia, R.A. Jiménez and J. Solà, *Phys. Lett.* **B347** (1995) 309; 321; **B351** (1995) 602(E).
- [25] D. Garcia, J. Solà, *Phys. Lett.* **B354** (1995) 335; **B357** (1995) 349.
- [26] A. Dabelstein, W. Hollik and W. Möslle, talk at *the Ringberg Workshop on "Perspectives for electroweak interactions in e^+e^- collisions"*, February 1995, hep-ph/9506251.
- [27] G.L. Kane, R.G. Stuart and J.D. Wells, *Phys. Lett.* **B354** (1995) 350.
- [28] P.H. Chankowski and S. Pokorski, *Phys. Lett.* **B356** (1995) 307.
- [29] M. Carena and C.E.M. Wagner, *Nucl. Phys.* **B452** (1995) 45; C.E.M. Wagner, talk at SUSY95, Palaiseau, France, May 1995, hep-ph/9510341.
- [30] X. Wang, J.L. Lopez and D.V. Nanopoulos, *Phys. Rev.* **D52** (1995) 4116.
- [31] E. Ma and D. Ng, Preprint TRI-PP-95-55, hep-ph/9508338.
- [32] J.D. Wells and G.L. Kane, Preprint SLAC-PUB-95-7038, hep-ph/9510372.
- [33] Y. Yamada, K. Hagiwara and S. Matsumoto, Talk by Y. Yamada at the *Yukawa International Seminar*, Kyoto, Japan, 20–25 Aug 1995, hep-ph/9512227.
- [34] R.S. Chivukula, S.B. Selipsky, and E.H. Simmons, *Phys. Rev. Lett.* **69** (1992) 575; R.S. Chivukula, E. Gates, E.H. Simmons, and J. Terning, *Phys. Lett.* **B311** (1993) 157.
- [35] N. Evans, *Phys. Lett.* **B331** (1994) 378.
- [36] N. Kitazawa, *Phys. Lett.* **B313** (1993) 395.
- [37] G-H. Wu, *Phys. Rev. Lett.* **74** (1995) 4137.
- [38] C-X. Yue, Y-P. Kuang, G-R. Lu and L-D. Wan, *Phys. Rev.* **D52** (1995) 5314.
- [39] K. Hagiwara and N. Kitazawa, *Phys. Rev.* **D52** (1995) 5374.

- [40] T. Yoshikawa, Preprint HUPD-9514 (1995), hep-ph/9506411; Talk at the *Yukawa International Seminar*, Kyoto, Japan, 20–25 Aug 1995.
- [41] R.S. Chivukula, E.H. Simmons, and J. Terning, *Phys. Lett.* **B331** (1994) 383.
- [42] B. Holdom, *Phys. Lett.* **B339** (1994) 114; *ibid.* **351** (1995) 279.
- [43] M. Peskin, Comment at the *Yukawa International Seminar*, Kyoto, Japan, 20–25 Aug 1995.
- [44] S. Dimopoulos and H. Georgi, *Nucl. Phys.* **B193** (1981) 150;
N. Sakai, *Z. Phys.* **C11** (1981) 153.
- [45] A. Masiero, D.V. Nanopoulos, K. Tamvakis, and T. Yanagida, *Phys. Lett.* **115B** (1982) 380.
- [46] K. Hagiwara and Y. Yamada, *Phys. Rev. Lett.* **70** (1992) 709;
Y. Yamada, *Z. Phys.* **C60** (1993) 83.
- [47] J. Bagger, K. Matchev and D. Pierce, *Phys. Lett.* **B348** (1995) 443.
- [48] J.L. Lopez and D.V. Nanopoulos, CTP-TAMU-29-95, hep-ph/9508253.
- [49] J. Ellis, in these proceedings.
- [50] K. Hagiwara, S. Matsumoto and Y. Yamada, in preparation.
- [51] J.M. Cornwall and J. Papavassiliou, *Phys. Rev.* **D40** (1989) 3474;
J. Papavassiliou and K. Phillippides, *ibid.* **48**(1993)4225; *ibid.* **51**(1995)6364;
J. Papavassiliou, *ibid.* **50**(1994)5998.
- [52] G. Degrassi and A. Sirlin, *Nucl. Phys.* **B383** (1992) 73; *Phys. Rev.* **D46** (1992) 3104; G. Degrassi, B. Kniehl and A. Sirlin, *ibid.* **48**(1993)R3963.
- [53] D.C. Kennedy and B.W. Lynn, *Nucl. Phys.* **B322** (1989) 1.
- [54] K. Hagiwara, S. Matsumoto and R. Szalapski, *Phys. Lett.* **B357** (1995) 411.
- [55] A. Sirlin, *Phys. Rev.* **D22** (1980) 971.
- [56] A.D. Martin and D. Zeppenfeld, *Phys. Lett.* **B345** (1995) 558.
- [57] M.L. Swartz, Preprint SLAC-PUB-95-7001, hep-ph/9509248.
- [58] H. Burkhardt and B. Pietrzyk, *Phys. Lett.* **B356** (1995) 398.
- [59] B.A. Kniehl, *Nucl. Phys.* **B347** (1990) 86.
- [60] H. Burkhardt, F. Jegerlehner, G. Penso and C. Verzegnassi, *Z. Phys.* **C43** (1989) 497.
- [61] F. Jegerlehner, in *Testing the Standard Model*, eds. M. Cvetič and P. Langacker (World Scientific, 1991).
- [62] F. Jegerlehner, cited by B.A. Kniehl in *Proc. Europhysics Marseille 1993*, p.639.
- [63] R.B. Nevzorov, A.V. Novikov and M.I. Vysotsky, *JETP Lett.* **60**(1994)399.
- [64] B.V. Geshkenbein and V.L. Morgunov, *Phys. Lett.* **B340** (1994) 185.
- [65] B.V. Geshkenbein and V.L. Morgunov, *Phys. Lett.* **B352** (1995) 456.
- [66] T. Takeuchi, Talk at the *Yukawa International Seminar*, Kyoto, Japan, 20–25 Aug 1995.
- [67] K. Hagiwara, D. Haidt and S. Matsumoto, to be published.
- [68] K. McFarland, Talk at the *XV Workshop on Weak Interactions and Neutrinos*, Talloires, France, 4–8 Sep 1995.

- [69] T. Appelquist and J. Terning, *Phys. Lett.* **B315** (1993) 139; *Phys. Rev.* **D50** (1994) 2116.
- [70] V.A. Novikov, L.B. Okun and M.I. Vysotsky, *Mod. Phys. Lett.* **A8** (1993) 2529; Erratum **A8**(1993)3301.
- [71] G.L. Fogli and D. Haidt, *Z. Phys.* **C40** (1988) 379.
- [72] P. Langacker, in *Precision Tests of the Standard Electroweak Model*, ed. by P. Langacker (World Scientific, 1994).
- [73] K. Kleinknecht, Talk presented at the *XXXth Rencontre de Moriond “Electroweak interactions and unified theories”*, Les Arcs, Savoie, 11–18 Mar 1995.
- [74] P.Gambio and A.Sirlin, *Phys. Rev. Lett.* **73** (1994) 621.
- [75] D. Amidei *et al.*, Preprint CDF/DOC/TOP/PUBLIC/3265 (Aug 1995).
- [76] S.I. Eidelman and V.N. Ivanchenko, *3’rd Workshop on Tau Lepton Physics*, Montreux, Switzerland, 19–22 Sep 1994, *Nucl. Phys. Proc. Suppl.* **40**(1995)131.
- [77] V.A.Novikov, L.B.Okun, A.N.Rozanov and M.I.Vysotsky, *Mod. Phys. Lett.* **A9** (1994) 2641; Z.Hioki, *Phys. Lett.* **B340** (1994) 181.